

Electronic Supporting Information

Pyrazine-Bridged Polynitro Triazoles for High Energy and Practical Stability

Abhishek Kumar Yadav,^a Richard J. Staples^b, Jean'ne M. Shreeve^{a*}

^aDepartment of Chemistry, University of Idaho, Moscow, Idaho 83844-2343, United States

*jshreeve@uidaho.edu

^bDepartment of Chemistry, Michigan State University, East Lansing, Michigan 48824, United States

Table of Contents

General Methods and synthesis of compounds	S1-S5
Crystal Structure analysis for 5	S5-S8
Copies of ¹ H, ¹³ C{ ¹ H} and IR spectra for 2	S9-S10
Copies of ¹ H, ¹³ C{ ¹ H} and IR spectra for 3	S10-S11
Copies of ¹ H, ¹³ C{ ¹ H} and IR spectra for 4	S12-S13
Copies of ¹ H and ¹³ C{ ¹ H} spectra, IR, and DSC plots for 5	S13-S15
Copies of ¹ H and ¹³ C{ ¹ H} and IR spectra for 6	S15-S16
Copies of ¹ H and ¹³ C{ ¹ H} spectra, IR, and DSC plots for 7	S17-S18
Copies of ¹ H and ¹³ C{ ¹ H} spectra, IR, and DSC plots for 7	S19-S20
Copies of ¹ H and ¹³ C{ ¹ H} spectra, IR, and DSC plots for 8	S21-S22
Computational details	S22-S25
References	S25-S26

Experimental Section:

Caution! The compounds in this work are energetic materials that could potentially explode under certain conditions (e.g., impact, friction, or electric discharge). Appropriate safety precautions, such as the use of shields in a fume hood and personal protection equipment (safety glasses, face shields, ear plugs, as well as gloves) should be always taken when handling these materials.

General. All reagents (analytical grade) were purchased from AK Scientific, VWR or Oakwood chemicals and were used as supplied. ^1H , ^{13}C , ^{14}N and ^{15}N NMR spectra were recorded using a 500 MHz (Bruker AVANCE 500) NMR spectrometer operating at 500.19, 125.78, 36.14, and 50.69 MHz, respectively. Chemical shifts in ^1H and ^{13}C NMR spectra are reported relative to Me_4Si ; ^{14}N and ^{15}N NMR spectra to MeNO_2 as an external standard. Abbreviations for multiplicities and descriptors are: s = singlet, br = broad, m = multiplet (denotes complex pattern), and q = quartet. The decomposition points (onset temperature) were obtained using a differential scanning calorimeter (TA Instruments Company, Model: Q2000). Infrared spectra were recorded on a FT-IR spectrometer (Thermo Nicolet 6700) equipped with an ATR assembly. The densities were measured at ambient temperatures by employing a gas pycnometer (Micromeritics AccuPyc II 1340). The impact and friction sensitivities were determined by using a standard BAM drop hammer and BAM friction tester, respectively. Elemental analyses were carried out on a Vario Micro cube Elementar Analyser.

Synthesis of pyrazine-2,5-dicarbohydrazide (2): Thionyl chloride (6 mL, 0.0713 mol) was added dropwise to a suspension of pyrazine-2,5-dicarboxylic acid (1) (2.0 g, 0.0118 mol) in ethanol (30 mL) at 0 °C. The resulting mixture was refluxed for 4 h, cooled to room temperature, and the solvent was evaporated under reduced pressure. A freshly prepared saturated solution of sodium acetate (12 mL) was then added to the residue, and the resulting precipitate was collected by filtration and washed with cold water. The solid obtained was dissolved in 80% hydrazine hydrate (10 mL) and heated in an oil bath at 70 °C for 4 h. After cooling to room temperature, the mixture was filtered, and the solid was washed with ethanol to afford compound **2** as a yellow solid. Yield (0.775 g, 0.003 mmol, 88.6%). ^1H NMR (500 MHz, DMSO- d_6): δ 10.27 (s, 2H), 9.10 (s, 2H), 4.68 (s, 4H). $^{13}\text{C}\{^1\text{H}\}$ NMR (126 MHz, DMSO- d_6) δ 154.3, 146.5, 141.6. IR (ATR ZnSe): $\tilde{\nu}$ 3308, 3087, 2953, 1691, 1578, 1512, 1436, 1332, 1275, 1214, 1179, 1088, 1023, 1006, 937, 864, 720 cm^{-1} . Elemental Analysis: Calcd for $\text{C}_6\text{H}_8\text{N}_6\text{O}_2$: C, 36.74; H, 4.11; N, 42.84. Found: C, 36.84; H, 4.09; N, 43.30.

Synthesis of diethyl 2,2'-(pyrazine-2,5-diylbis(1H-1,2,4-triazole-5,3-diyl))diacetate (3): Ethyl 3-ethoxy-3-iminopropanoate (6.0 g, 0.0306 mol) was dissolved in acetonitrile (30 mL), and triethylamine (2.06 g, 2.84 mL, 0.0232 mol) was added with stirring at room temperature for 30 min. Subsequently, compound **2** (1.0 g, 0.0050 mol) and glacial acetic acid (10 mL) were added, and the reaction mixture was refluxed for 15 h. After completion of the reaction, the excess solvent was evaporated, and water was added. The mixture was sonicated to afford a pale-yellow solid, which was collected and dried to give compound **3** (1.57 g, 0.0040 mol, 80%). ¹H NMR (500 MHz, DMSO-d₆): δ 9.29 (s, 2H), 4.15 (q, 4H), 3.87 (s, 4H), 1.21 (t, 6H). ¹³C{¹H} NMR (126 MHz, DMSO-d₆): 168.5, 160.6, 146.3, 141.8, 141.6, 60.7, 33.2, 13.9. IR (ATR ZnSe): $\tilde{\nu}$ 3435, 3309, 3235, 2985, 1739, 1691, 1578, 1512, 1462, 1368, 1269, 1213, 1165, 1088, 1061, 1029, 1003, 936, 868, 719 cm⁻¹. Elemental Analysis: Calcd for C₁₆H₁₈N₈O₄ (CH₃CN): C, 50.58; H, 4.95; N, 29.49. Found: C, 50.83; H, 4.87; N, 29.51.

Synthesis of 2,2'-(pyrazine-2,5-diylbis(1H-1,2,4-triazole-5,3-diyl))diacetic acid (4): Compound **3** (1.0 g, 0.0025 mol) was dissolved in an aqueous solution of sodium hydroxide (0.40 g, 0.0100 mol) in 12 mL of distilled water. The resulting mixture was stirred at 70 °C for 1 h, then cooled to 0 °C. Concentrated sulfuric acid was added dropwise to adjust the pH to approximately 3, and the mixture was stirred at room temperature. The resulting yellow precipitate was collected by filtration and dried at room temperature to afford pure compound **4** as a yellow solid. Yield (0.77 g, 0.0023 mol, 90%). ¹H NMR (500 MHz, DMSO-d₆): δ 9.29 (s, 2H), 3.86 (s, 4H). ¹³C{¹H} NMR (126 MHz, DMSO-d₆): δ 170.0, 155.6, 154.9, 143.5, 141.8, 33.3. IR (ATR ZnSe): $\tilde{\nu}$ 3177, 2925, 1721, 1548, 1462, 1389, 1267, 1192, 1059, 1032, 996, 923, 821, 821, 752 cm⁻¹. Elemental Analysis Calcd for C₁₂H₁₀N₈O₄: C, 43.64; H, 3.05; N, 33.93. Found: C, 43.75; H, 3.48; N, 34.01.

Synthesis of 2,5-bis(3-(trinitromethyl)-1H-1,2,4-triazol-5-yl)pyrazine (5, 1st method): Compound **4** (500 mg, 1.513 mmol) was added portion wise to the mixture of fuming nitric acid (3 mL) and 4 mL conc. sulfuric acid (98%) in ice-water bath at 0 °C. After addition, reaction mixture was stirred at same temperature for 20 mins, further stirred for 12 hrs at room temperature and poured into crushed ice with stirring. The precipitate was washed with water and dried in air to get white solid compound **5**. Yield (620 mg, 1.210 mmol, 80%). *T_d* (onset): 150 °C. ¹H NMR (500 MHz, DMSO-d₆): δ 9.44 (s, 2H). ¹³C NMR (126 MHz, DMSO-d₆) δ 154.7, 148.7, 142.5, 141.6, 122.7. IR (ATR ZnSe): $\tilde{\nu}$ 3384, 3178, 2884, 1772, 1595, 1488, 1437, 1338, 1283, 1165, 1081, 1049, 1006, 966, 843, 801, 743, 682, 646 cm⁻¹. Elemental

Analysis Calcd for C₁₀H₄N₁₄O₁₂ : C, 23.45; H, 0.79; N, 38.28. Found: C, 23.46; H, 1.10; N, 37.76.

Synthesis of diethyl 2,2'-(pyrazine-2,5-diylbis(1H-1,2,4-triazole-5,3-diyl))bis(2,2-dinitroacetate) (6): Compound **3** (500 mg, 1.294 mmol) was added portion wise to the mixture of fuming nitric acid (3 mL) and 4 mL conc. sulfuric acid (98%) in an ice-water bath at 0 °C. After addition, the reaction mixture was stirred at same temperature for 20 mins, further stirred for 12 hrs at room temperature and poured into crushed ice with stirring. The precipitate was washed with water and dried in air to get white solid compound **6**. Yield (601 mg, 1.061 mmol, 82%). ¹H NMR (500 MHz, DMSO-d₆): δ 9.40 (s, 2H), 4.65 (q, 4H), 1.36 (t, 6H). ¹³C NMR (126 MHz, DMSO-d₆) δ 156.1, 153.9, 151.8, 142.3, 141.7, 113.6, 66.8, 13.4. IR (ATR ZnSe): $\tilde{\nu}$ 3383, 3186, 2982, 1772, 1585, 1470, 1440, 1372, 1301, 1243, 1160, 1080, 1037, 1004, 952, 847, 801, 748, 723 cm⁻¹. Elemental Analysis Calcd for C₁₆H₁₄N₁₂O₁₂ : C, 33.93; H, 2.49; N, 29.68. Found: C, 33.75; H, 2.58; N, 29.96.

General procedure for the synthesis of salts 7-9

Ammonia (35 mg, 0.998 mmol) or hydrazine hydrate (50 mg, 0.998 mmol), or hydroxylamine hydrate (33 mg, 0.999 mmol), was slowly added to compound **5** (200 mg, 0.390 mmol) or **6** (200 mg, 0.353 mmol) in methanol (5 mL) at room temperature. After stirring for 6 hrs at room temperature, the precipitate was collected by filtration and dried in air to give the desired products in quantitative yields. However, despite using an excess of base to obtain the tetracationic salts, we did not achieve the desired product; instead, the reactions yielded the dicationic salts **7–9**.

Diammonium (pyrazine-2,5-diylbis(1H-1,2,4-triazole-5,3-diyl))bis(dinitromethanide) (7): Yield: (145 mg, 0.317 mmol, 90%) as a yellow solid. *T_d* (onset): 205 °C. ¹H NMR (500 MHz, DMSO-d₆): δ 9.32 (s, 2H), 6.15 (s, 8H). ¹³C NMR (126 MHz, DMSO-d₆) δ 156.9, 151.2, 144.2, 141.9, 124.8. IR (ATR ZnSe): $\tilde{\nu}$ 3354, 3222, 3097, 1628, 1520, 1479, 1442, 1393, 1349, 1256, 1176, 1129, 1074, 1037, 995, 940, 831, 751, 686, 482 cm⁻¹. Elemental Analysis Calculated for C₁₀H₁₂N₁₄O₈: C, 26.32; H, 2.65; N, 42.98. Found: C, 26.77; H, 3.00; N, 43.47.

Dihydrazinium (pyrazine-2,5-diylbis(1H-1,2,4-triazole-5,3-diyl))bis(dinitromethanide) (8): Yield: (156 mg, 0.320 mmol, 91%) as a yellow solid. *T_d* (onset): 215 °C. ¹H NMR (500 MHz, DMSO-d₆): δ 9.32 (s, 2H), 5.23 (s, 10H). ¹³C NMR (126 MHz, DMSO-d₆) δ 156.9, 151.1, 144.2, 141.9, 124.7. IR (ATR ZnSe): $\tilde{\nu}$ 3342, 3259, 2917, 2643, 1622, 1532, 1488, 1451, 1399,

1355, 1271, 1225, 1171, 1091, 1032, 999, 977, 826, 748, 684 cm⁻¹. Elemental Analysis Calculated for C₁₀H₁₄N₁₆O₈: C, 24.70; H, 2.90; N, 46.08. Found: C, 24.62; H, 3.46; N, 45.77.

Dihydroxyl ammonium (pyrazine-2,5-diylbis(1H-1,2,4-triazole-5,3-diyl))bis(dinitromethanide) (9): Yield: (150 mg, 0.307 mmol, 87%) as a yellow solid. *T*_d (onset): 210 °C. ¹H NMR (500 MHz, DMSO-d₆): δ 9.31 (s, 2H), 3.55 (broad, NH₃OH⁺, overlapped with residual water signal of DMSO-d₆). ¹³C NMR (126 MHz, DMSO-d₆) δ 156.9, 151.1, 144.2, 141.9, 124.6. IR (ATR ZnSe): $\tilde{\nu}$ 3447, 2721, 1640, 1536, 1492, 1454, 1398, 1362, 1276, 1236, 1203, 1174, 1129, 1096, 1032, 1000, 828, 747, 678, 519 cm⁻¹. Elemental Analysis Calculated for C₁₀H₁₂N₁₄O₁₀: C, 24.60; H, 2.48; N, 40.16. Found: C, 24.74; H, 2.97; N, 40.36.

Synthesis of 2,5-bis(3-(trinitromethyl)-1H-1,2,4-triazol-5-yl)pyrazine (5, 2nd method) from ammonium salt 7: Compound 7 (500.0 mg, 1.095 mmol) was added portion wise to a stirred mixture of fuming nitric acid (3.0 mL) and concentrated sulfuric acid (4.0 mL, 98%) in an ice–water bath at 0 °C. After the addition was complete, the reaction mixture was stirred at 0 °C for 20 min, then allowed to warm and stirred at room temperature for 12 h. The reaction mixture was quenched by pouring onto crushed ice with stirring. The resulting precipitate was collected, washed with water, and dried in air to give the white solid **5** in 78% yield. All characterisation data matched well with those of compound **5** prepared by the first method.

X-ray crystallographic details and crystallographic data Section

Sample preparation:

Single crystals of compound **5** suitable for single-crystal X-ray analysis were obtained from methanol solution.

Data collection:

A suitable crystal with dimensions 0.17 × 0.14 × 0.09 mm³ was selected and mounted on a nylon loop with Paratone oil on a XtaLAB Synergy, Dualflex, HyPix diffractometer. The crystal was kept at a steady *T* = 100.00(10) K during data collection. The structure was solved with the ShelXT¹ solution program using dual methods and by using Olex2.² The model was refined with ShelXL³ using full matrix least squares minimisation on *F*². The thermal ellipsoids and packing diagrams of X-ray structures in the main article and supplementary material are plotted using Olex 2 software.²

Crystal structures and crystallographic data

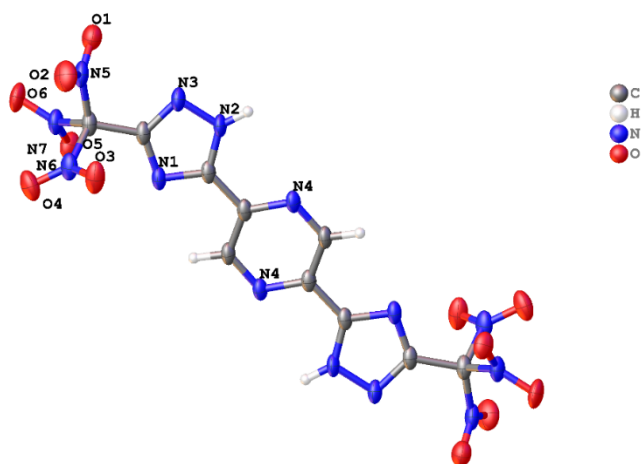


Figure S1. Crystal structure of compound **5**, drawing at 50% ellipsoid showing the labelling of the hetero atoms.

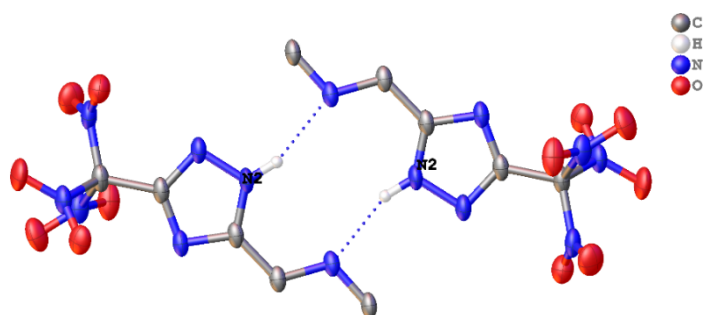


Figure S2. The following hydrogen bonding interactions with a maximum D-D distance of 3.1 Å and a minimum angle of 110 ° are present in JS825H: N2–N4₁: 2.888 Å.

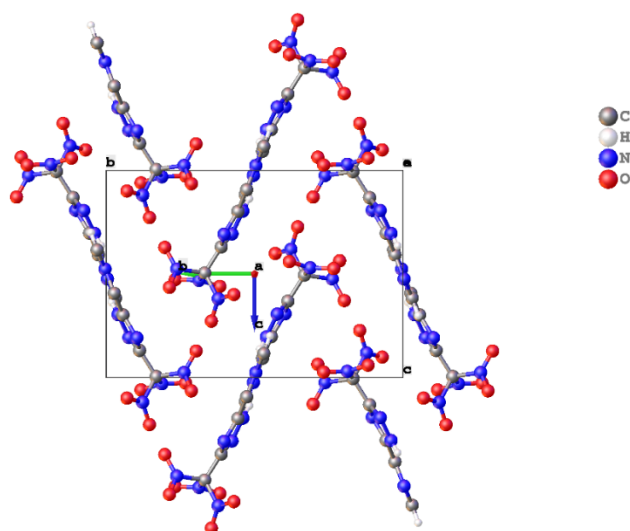


Figure S3. Packing diagram of **5** viewed along the *c*-axis.

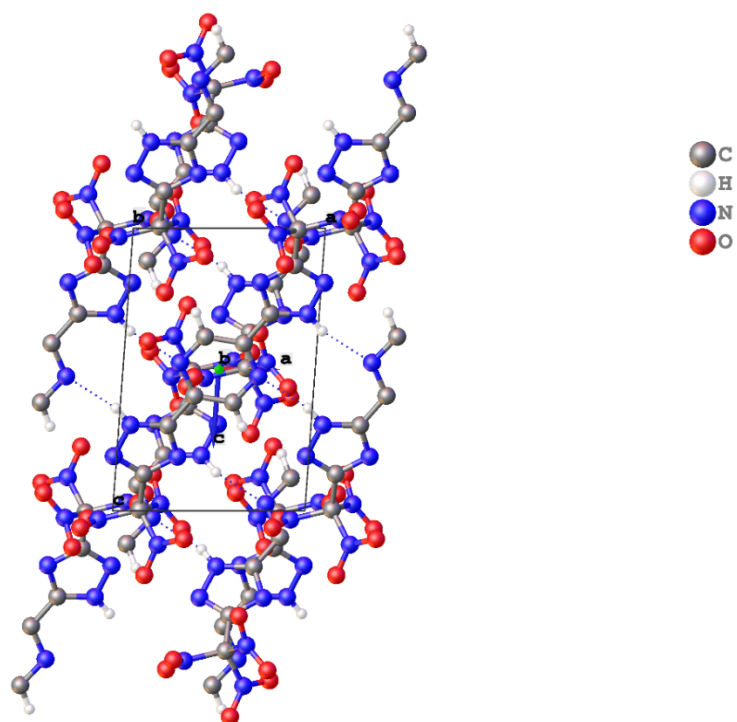


Figure S4. Packing diagram of **5** viewed along the *b*-axis.

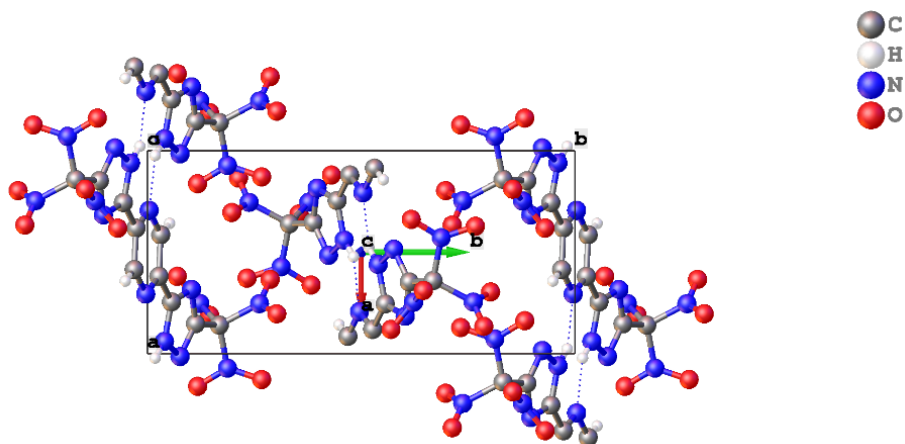


Figure S5. Packing diagram of **5** viewed along the *c*-axis.

Table S1: Crystallographic data for **5**.

Compound	5
CCDC No.	2497606
Formula	C ₁₀ H ₄ N ₁₄ O ₁₂
<i>D</i> _{calc.} / g cm ⁻³	1.772
<i>m</i> /mm ⁻¹	1.452
Formula Weight	512.27
Colour	colourless
Shape	block-shaped
Size/mm ³	0.17×0.14×0.09
<i>T</i> /K	99.99(10)
Crystal System	monoclinic
Space Group	<i>P</i> 2 ₁ / <i>n</i>
<i>a</i> /Å	6.76375(14)
<i>b</i> /Å	14.2639(3)
<i>c</i> /Å	9.97845(16)
<i>a</i> [°]	90
<i>b</i> [°]	94.1732(18)
<i>g</i> [°]	90
<i>V</i> /Å ³	960.14(3)
<i>Z</i>	2
<i>Z</i> '	0.5
Wavelength/Å	1.54184
Radiation type	Cu K _α
<i>Q</i> _{min} [°]	5.420
<i>Q</i> _{max} [°]	79.901
Measured Refl's.	8284
Indep't Refl's	2046
Refl's I ≥ 2 <i>s</i> (I)	1909
<i>R</i> _{int}	0.0273
Parameters	171
Restraints	0
Largest Peak	0.237
Deepest Hole	-0.246
GooF	1.097
<i>wR</i> ₂ (all data)	0.1089
<i>wR</i> ₂	0.1073
<i>R</i> _I (all data)	0.0432
<i>R</i> _I	0.0408

Copies of ^1H , $^{13}\text{C}\{^1\text{H}\}$ and ^{14}N spectra, IR, and DSC plots

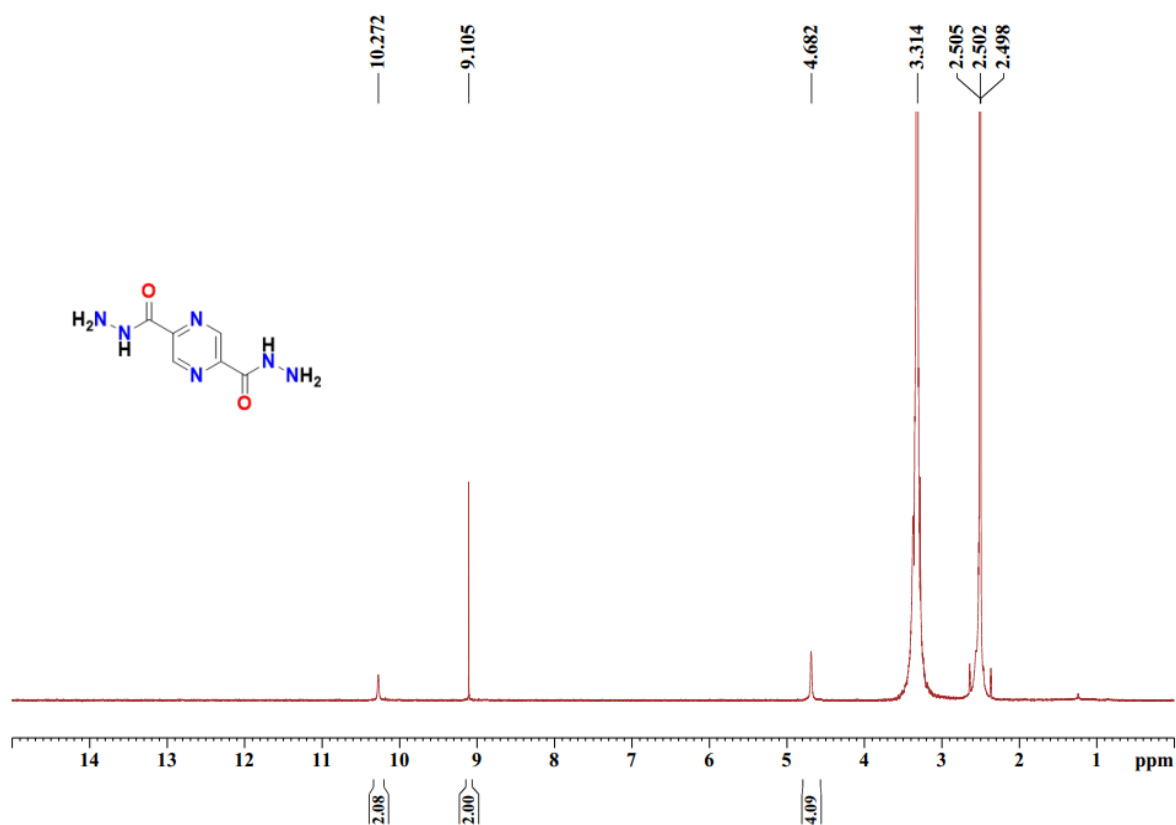


Figure S6: ^1H NMR Spectrum of compound 2 (recorded in DMSO- d_6 ; 500 MHz).

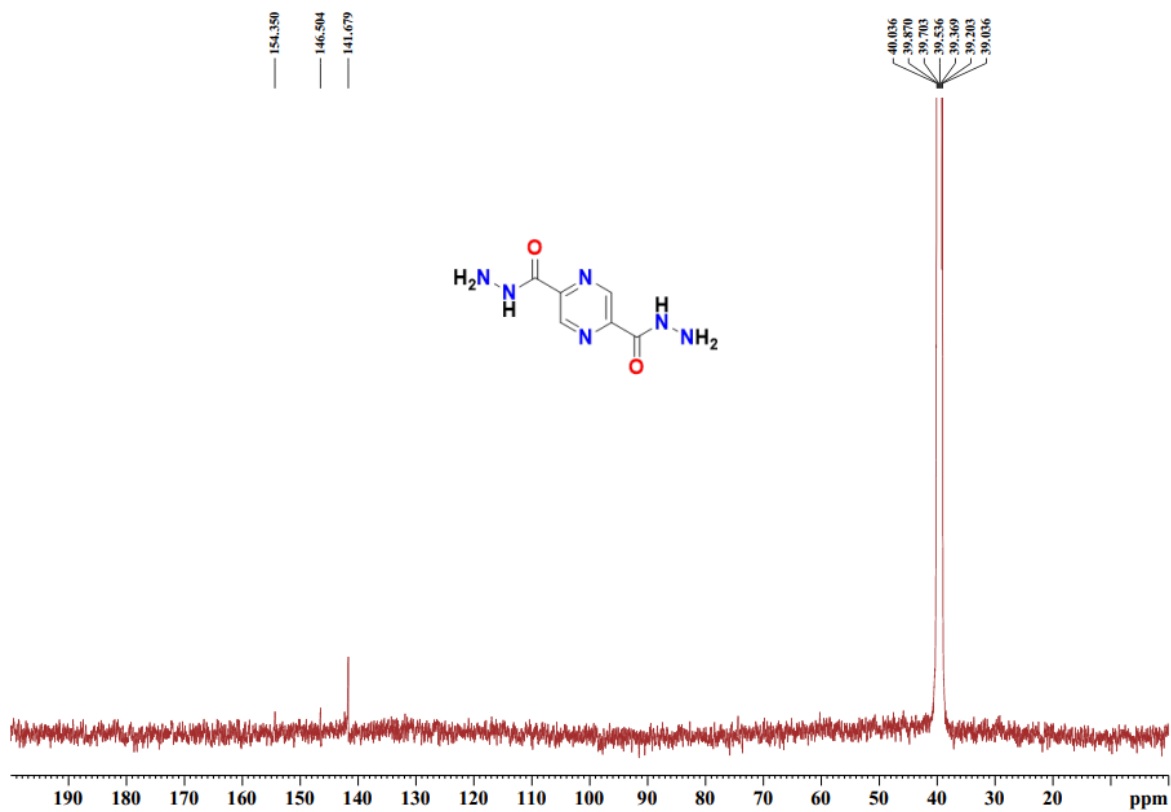


Figure S7: $^{13}\text{C}\{^1\text{H}\}$ NMR Spectrum of compound 2 (recorded in DMSO- d_6 ; 126 MHz).

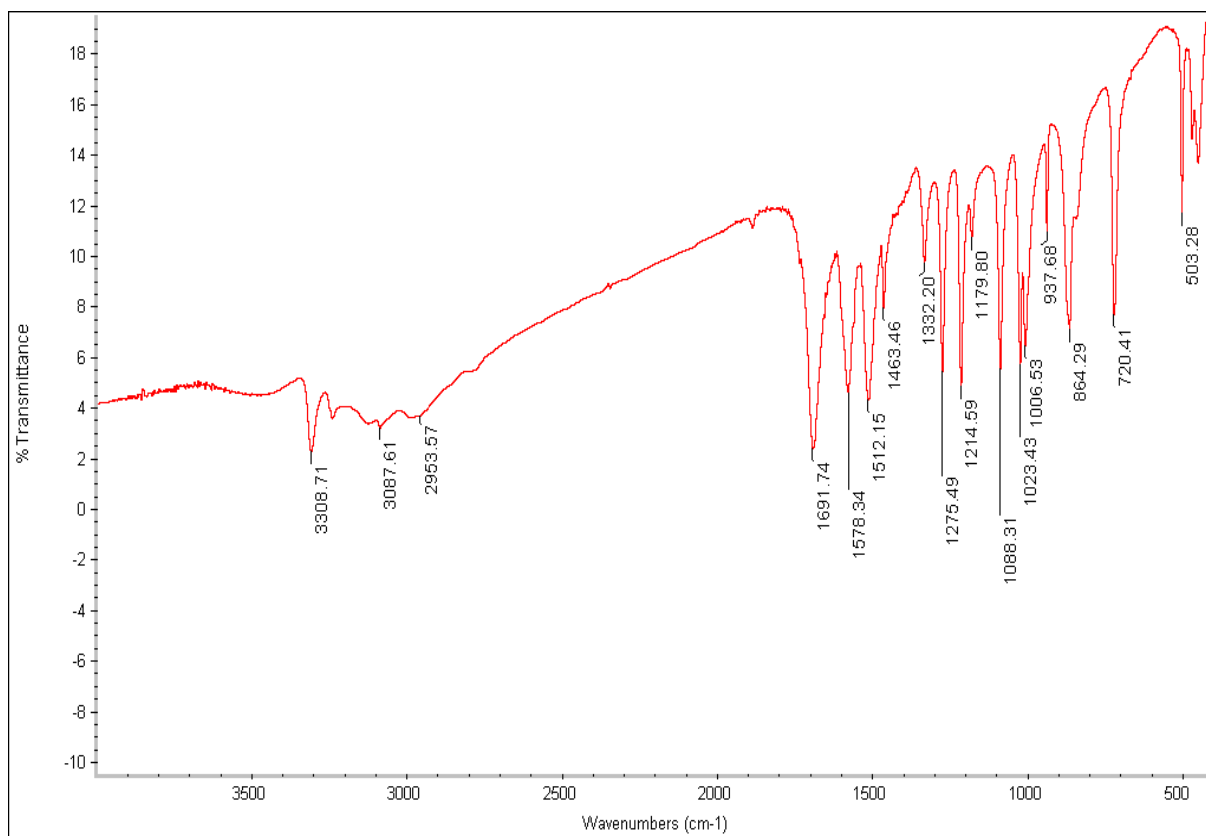


Figure S8: IR Spectrum of compound 2.

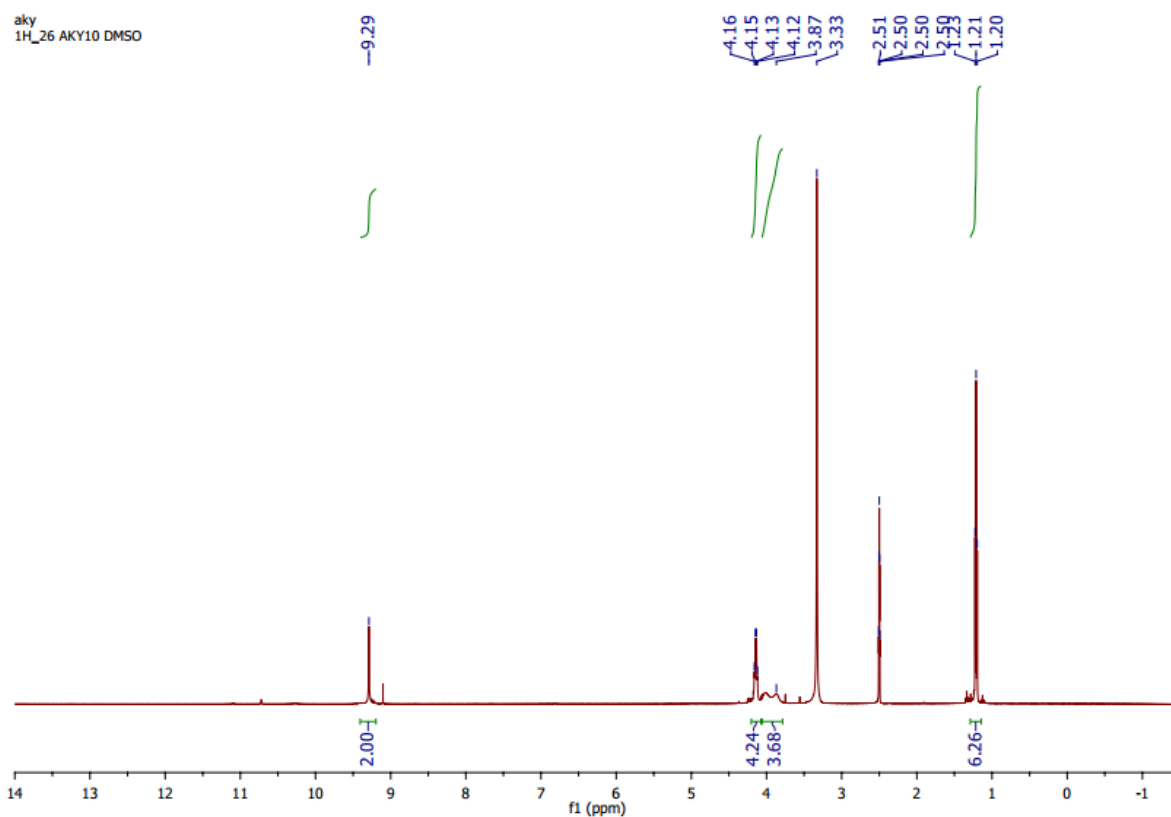


Figure S9: ¹H NMR Spectrum of compound 3 (recorded in DMSO-d₆; 500 MHz).

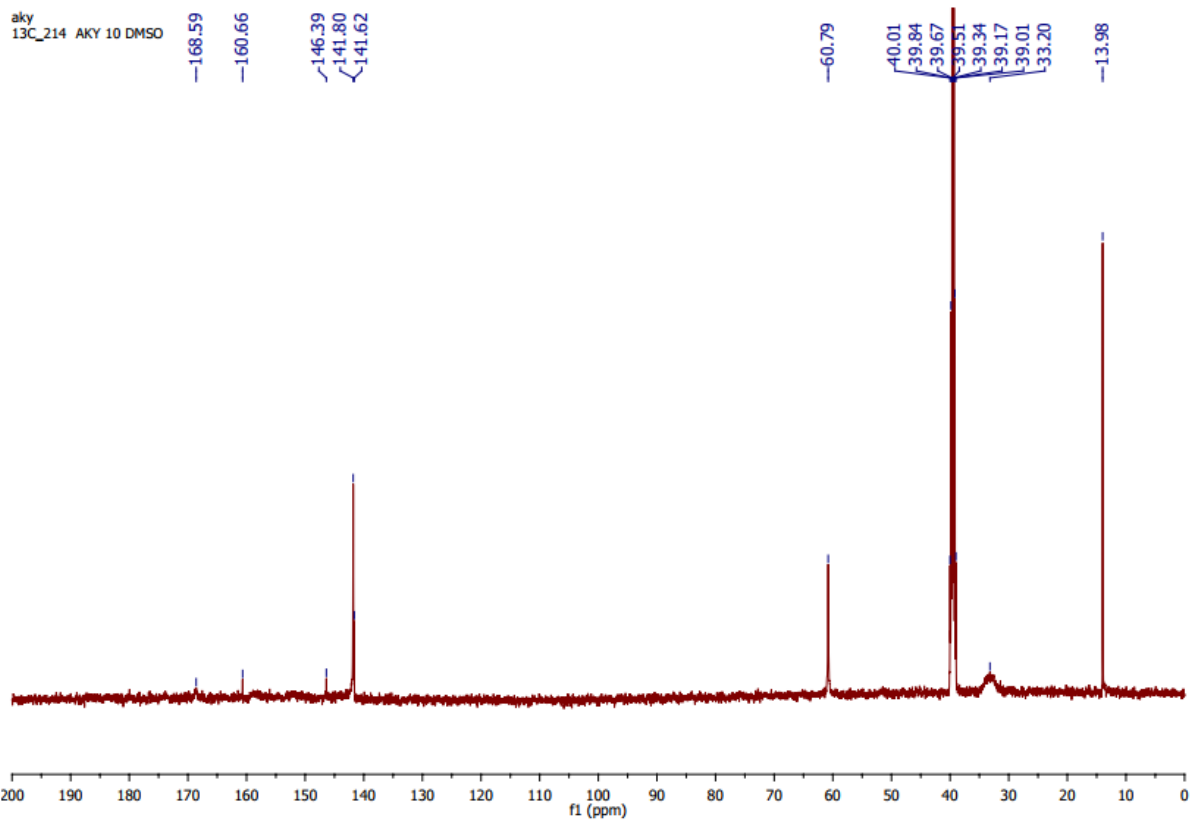


Figure S10: $^{13}\text{C}\{^1\text{H}\}$ NMR Spectrum of compound 3 (recorded in DMSO- d_6 ; 126 MHz).

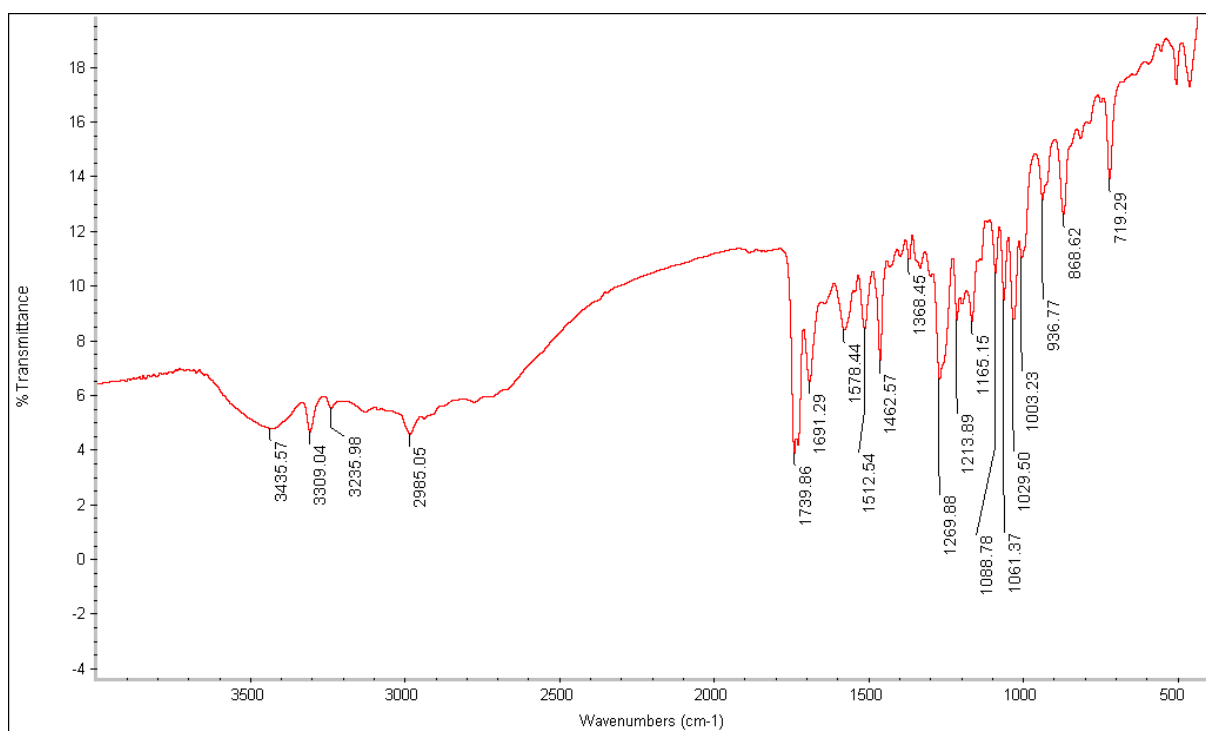


Figure S11: IR Spectrum of compound 3.

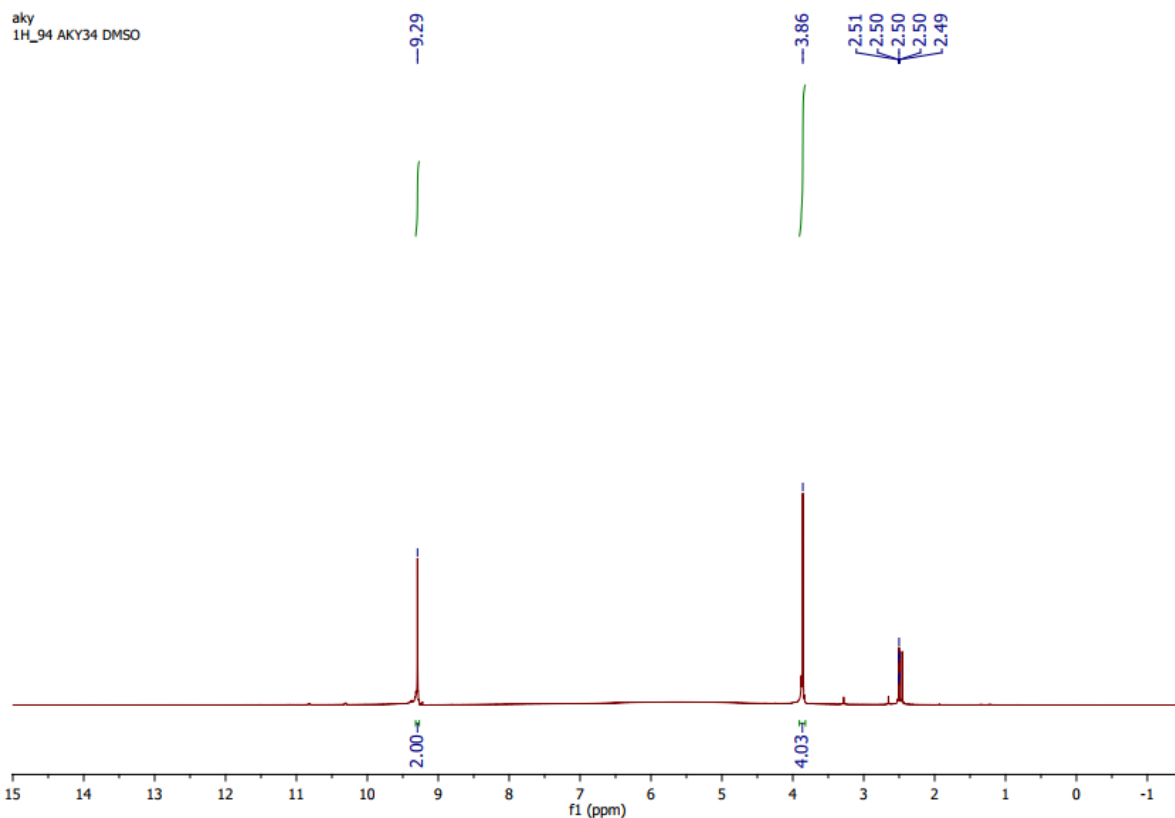


Figure S12: ^1H NMR Spectrum of compound 4 (recorded in DMSO-d₆; 500 MHz).

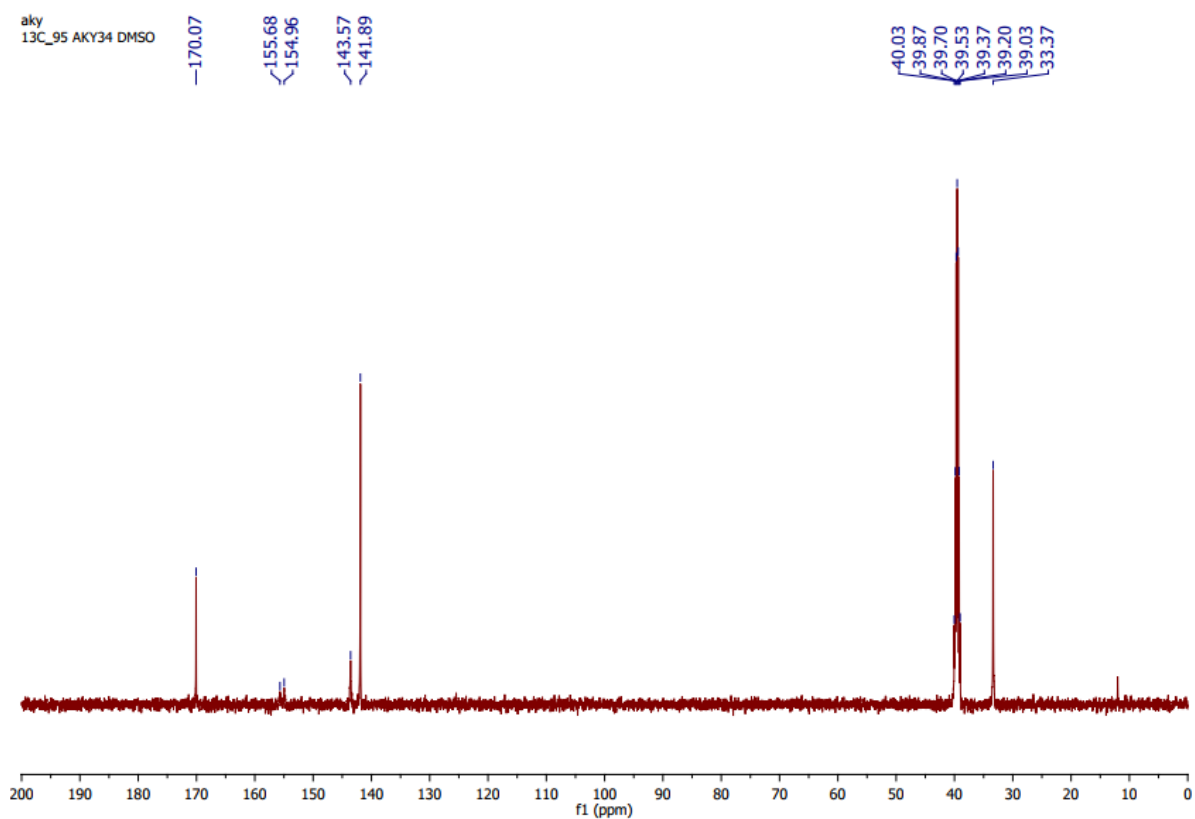


Figure S13: $^{13}\text{C}\{^1\text{H}\}$ NMR Spectrum of compound 4 (recorded in DMSO-d₆; 126 MHz).

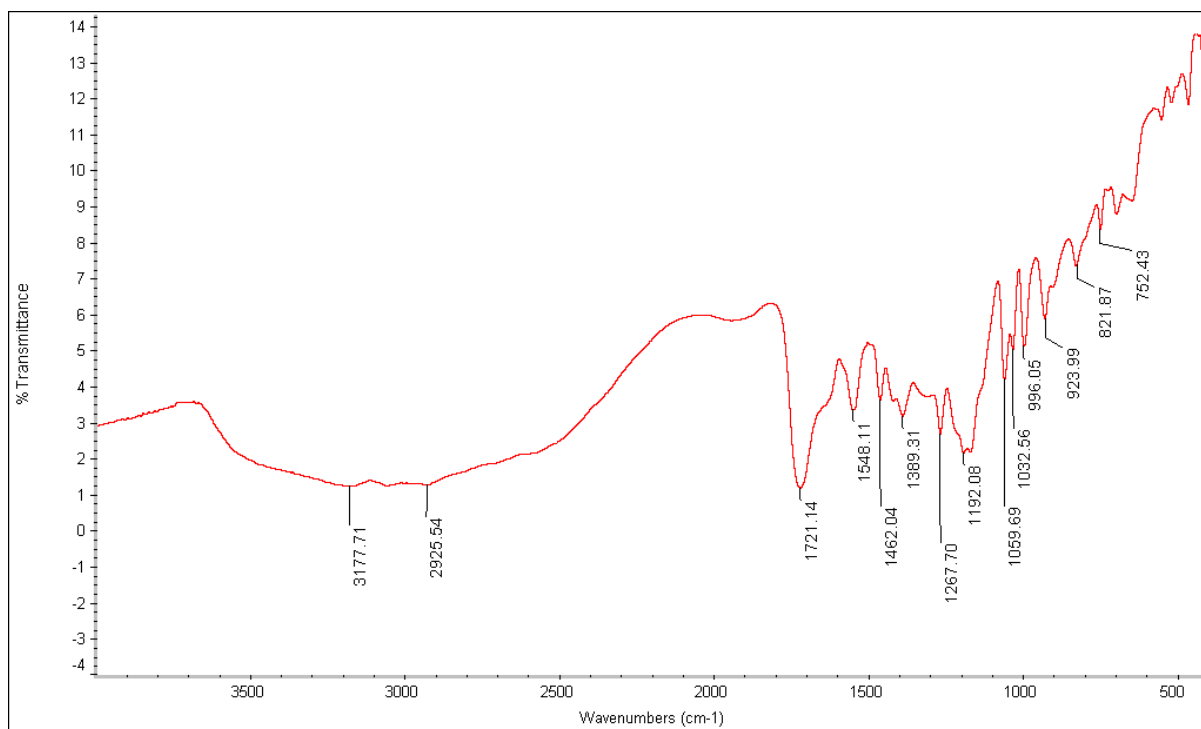


Figure S14: IR Spectrum of compound 4.

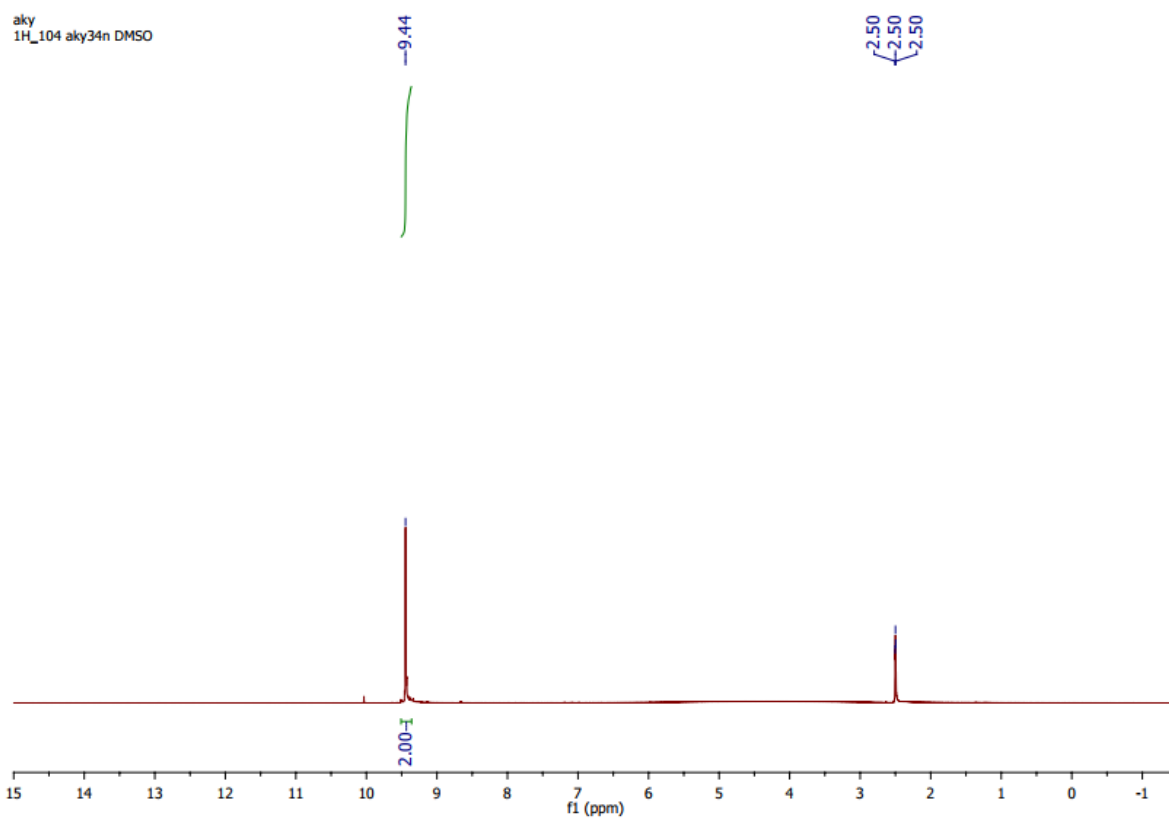


Figure S15: ^1H NMR Spectrum of compound 5 (recorded in DMSO- d_6 ; 500 MHz).

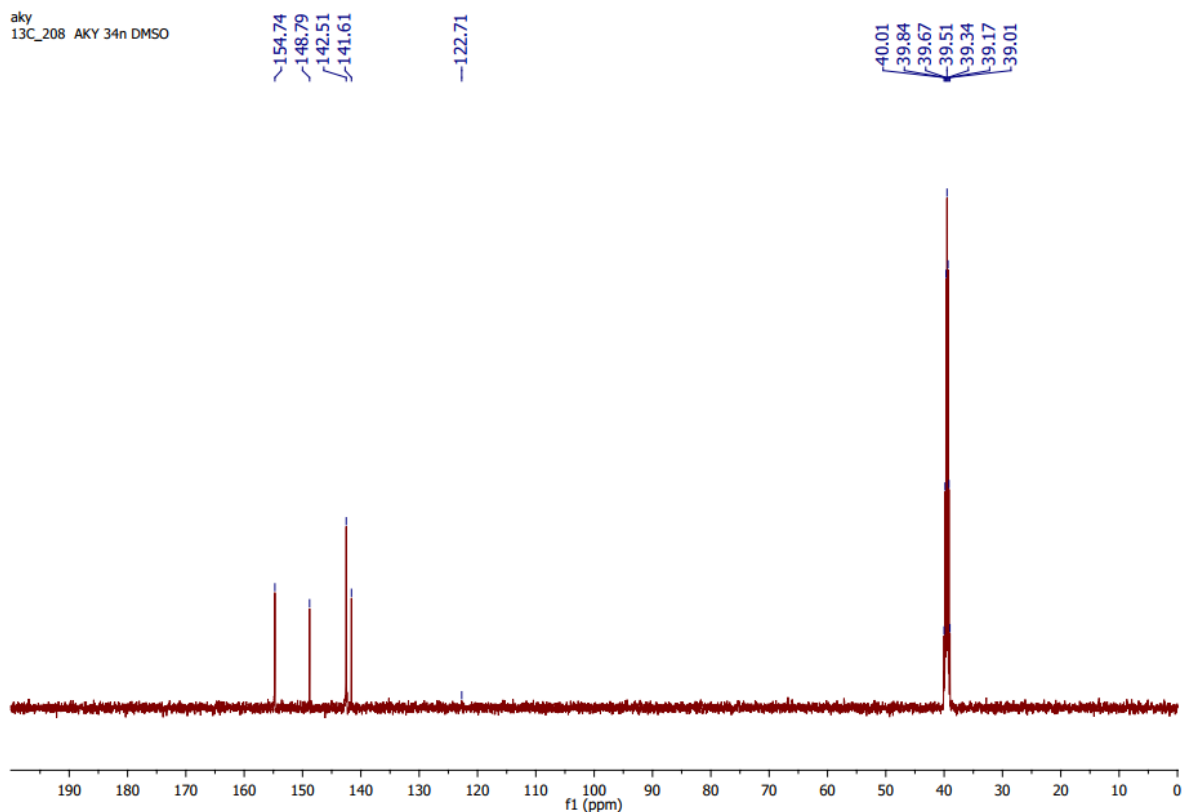


Figure S16: $^{13}\text{C}\{^1\text{H}\}$ NMR Spectrum of compound 5 (recorded in DMSO- d_6 ; 126 MHz).

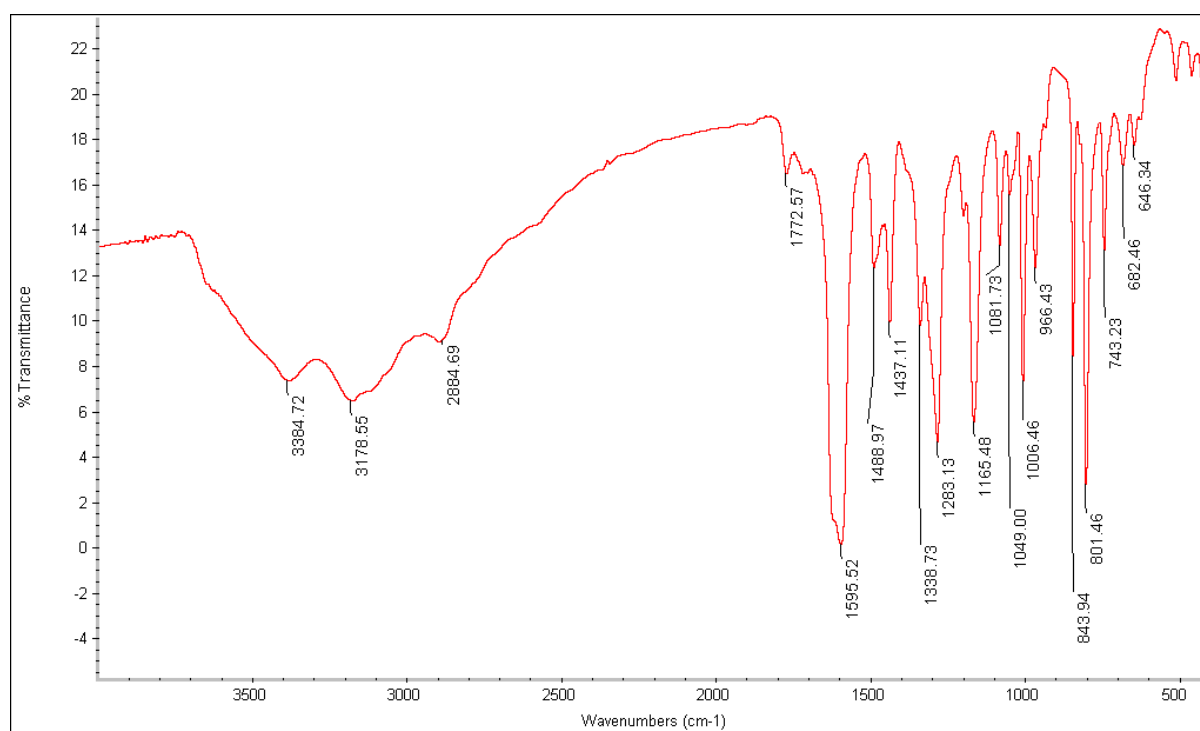


Figure S17: IR Spectrum of compound 5.

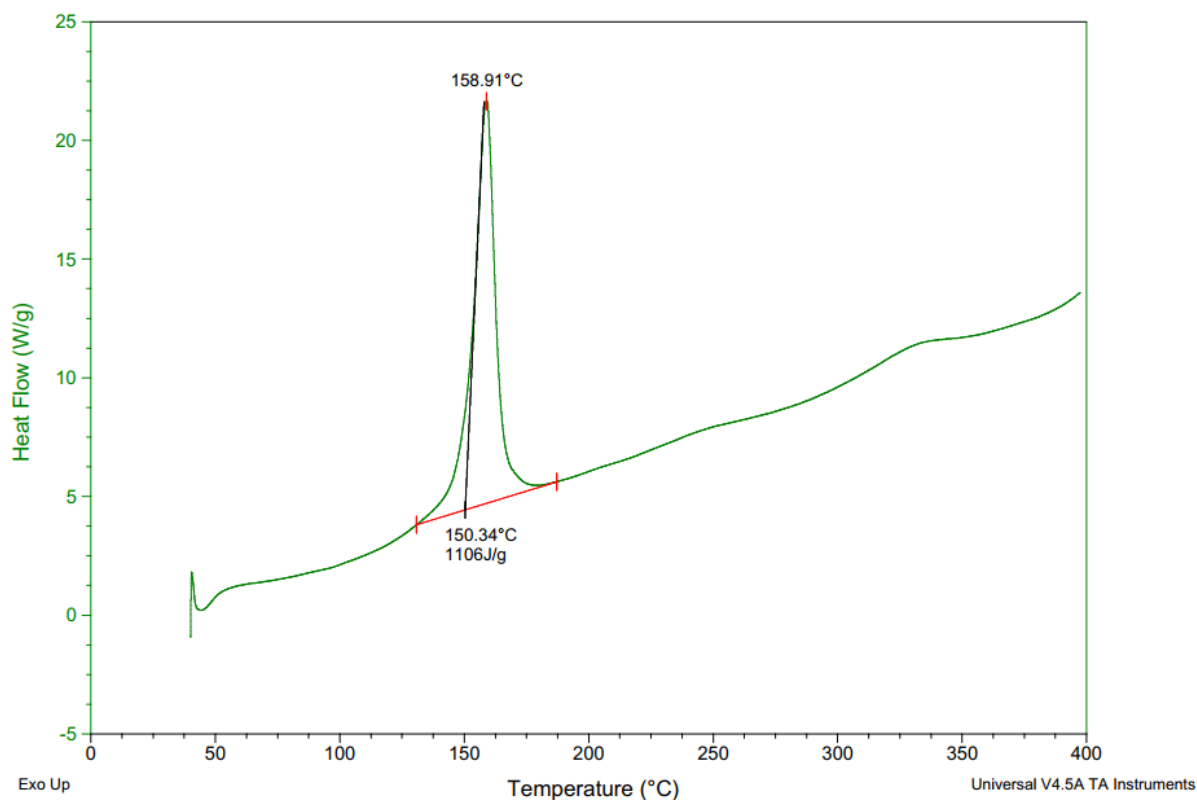


Figure S18. DSC Plot of compound 5 at Heating rate 5 °C min⁻¹.

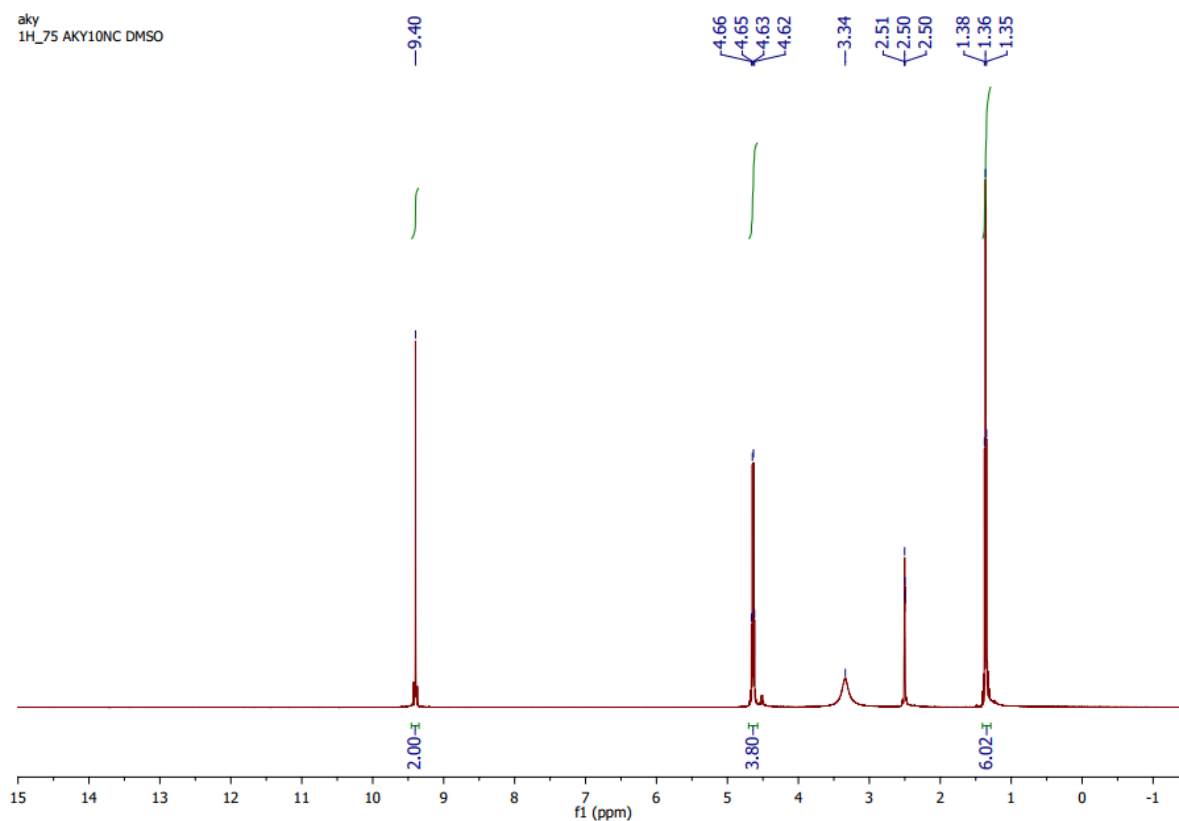


Figure S19: ¹H NMR Spectrum of compound 6 (recorded in DMSO-d₆; 500 MHz).

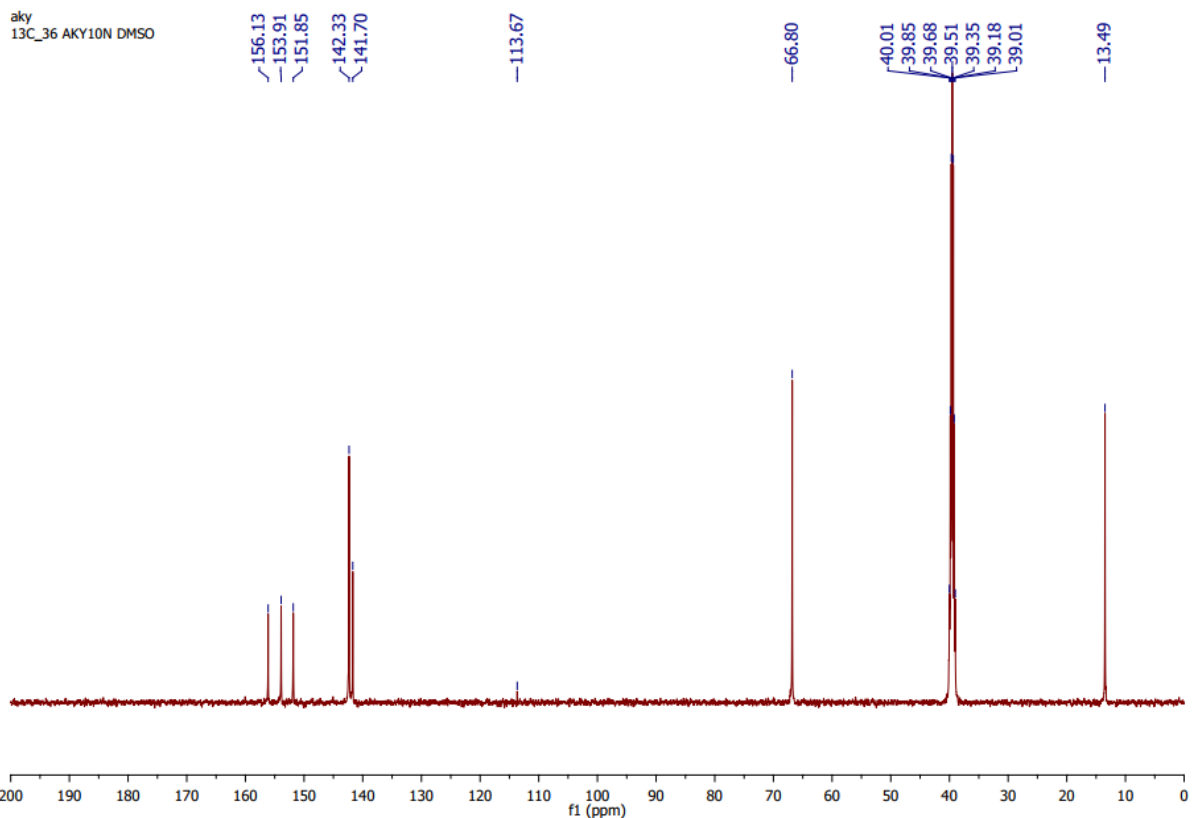


Figure S20: $^{13}\text{C}\{^1\text{H}\}$ NMR Spectrum of compound 6 (recorded in DMSO-d₆; 126 MHz).

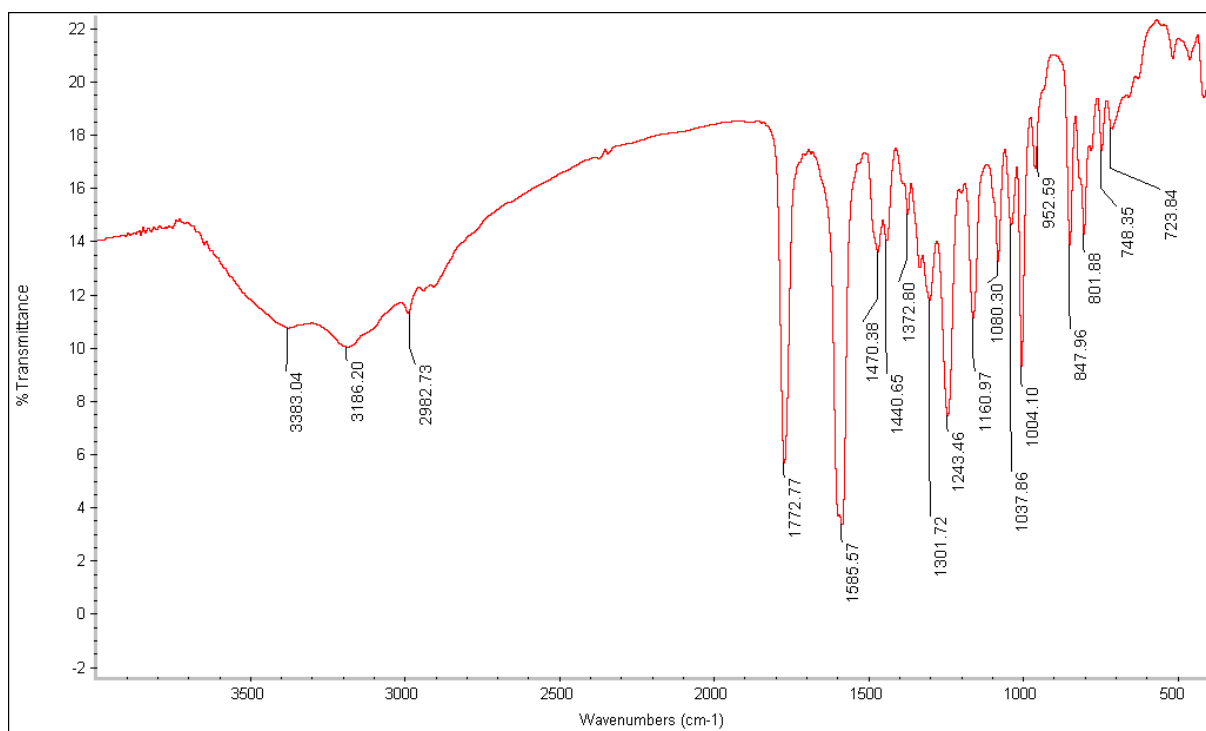


Figure S21: IR Spectrum of compound 6.

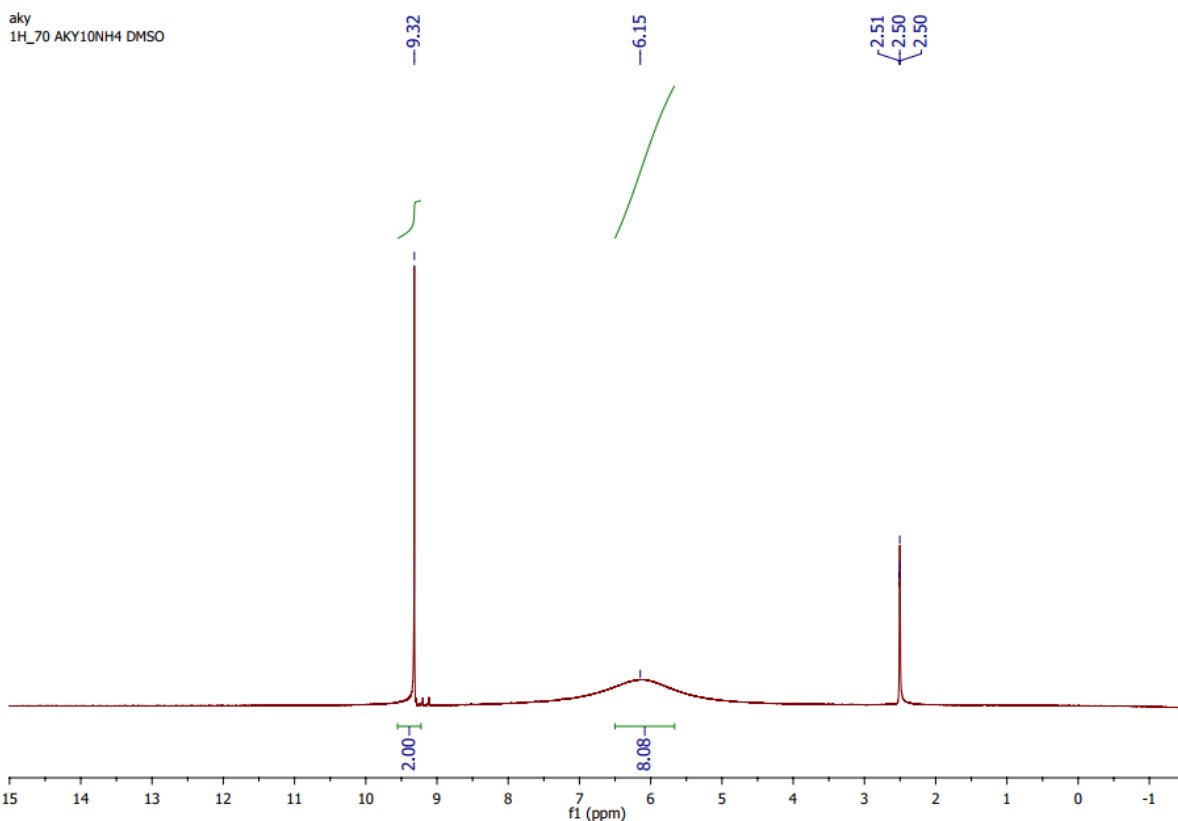


Figure S22: ^1H NMR Spectrum of compound 7 (recorded in DMSO-d₆; 500 MHz).

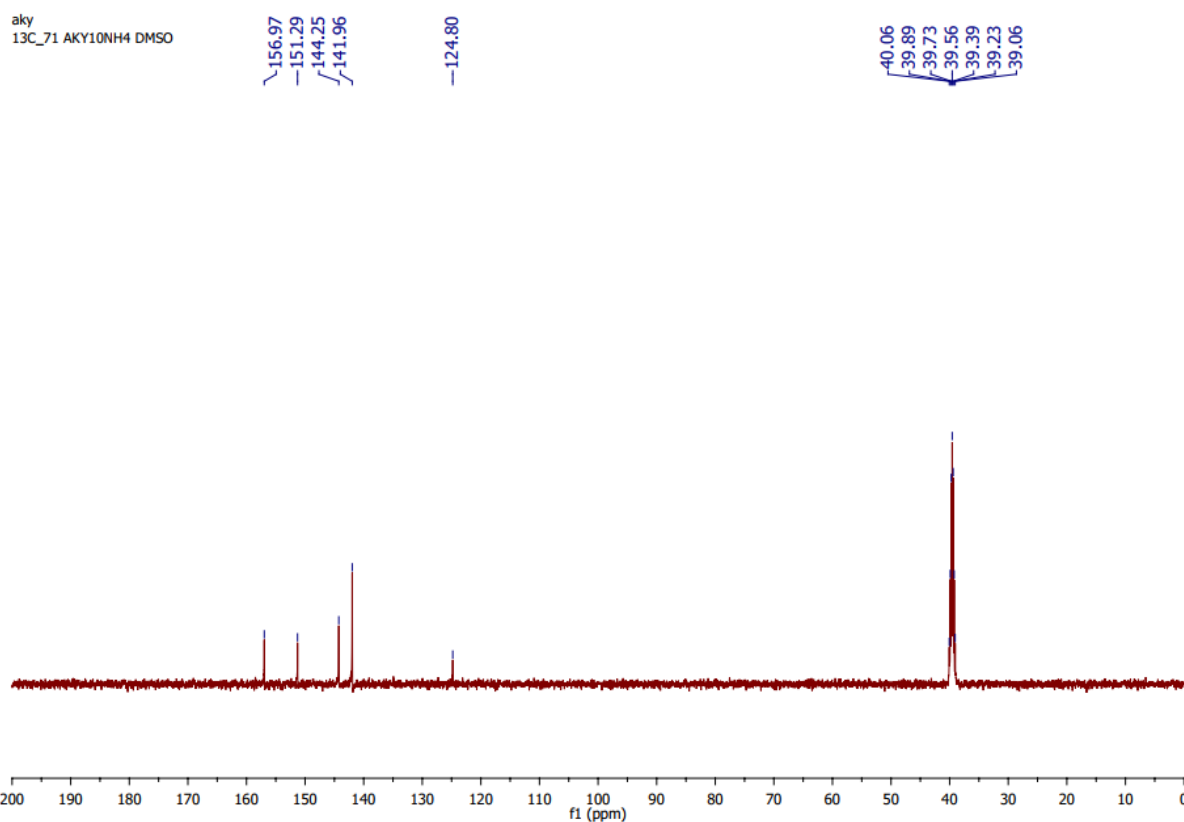


Figure S23: $^{13}\text{C}\{^1\text{H}\}$ NMR Spectrum of compound 7 (recorded in DMSO-d₆; 126 MHz).

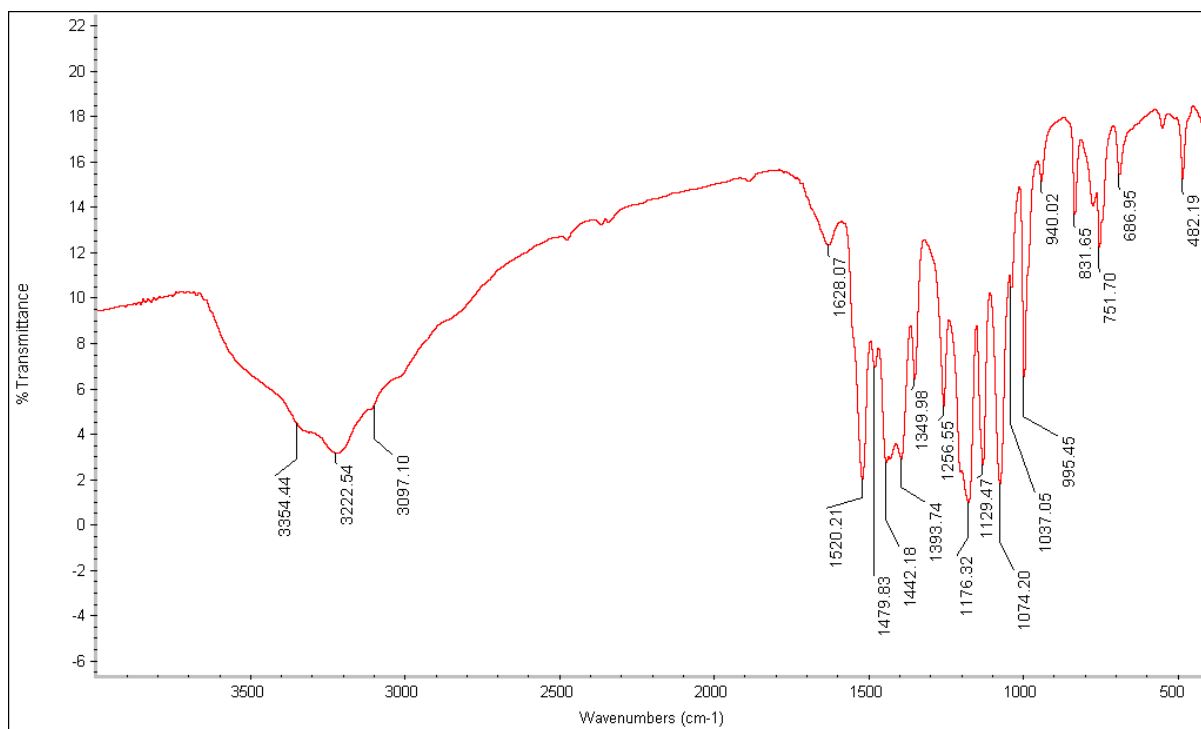


Figure S24: IR Spectrum of compound 7.

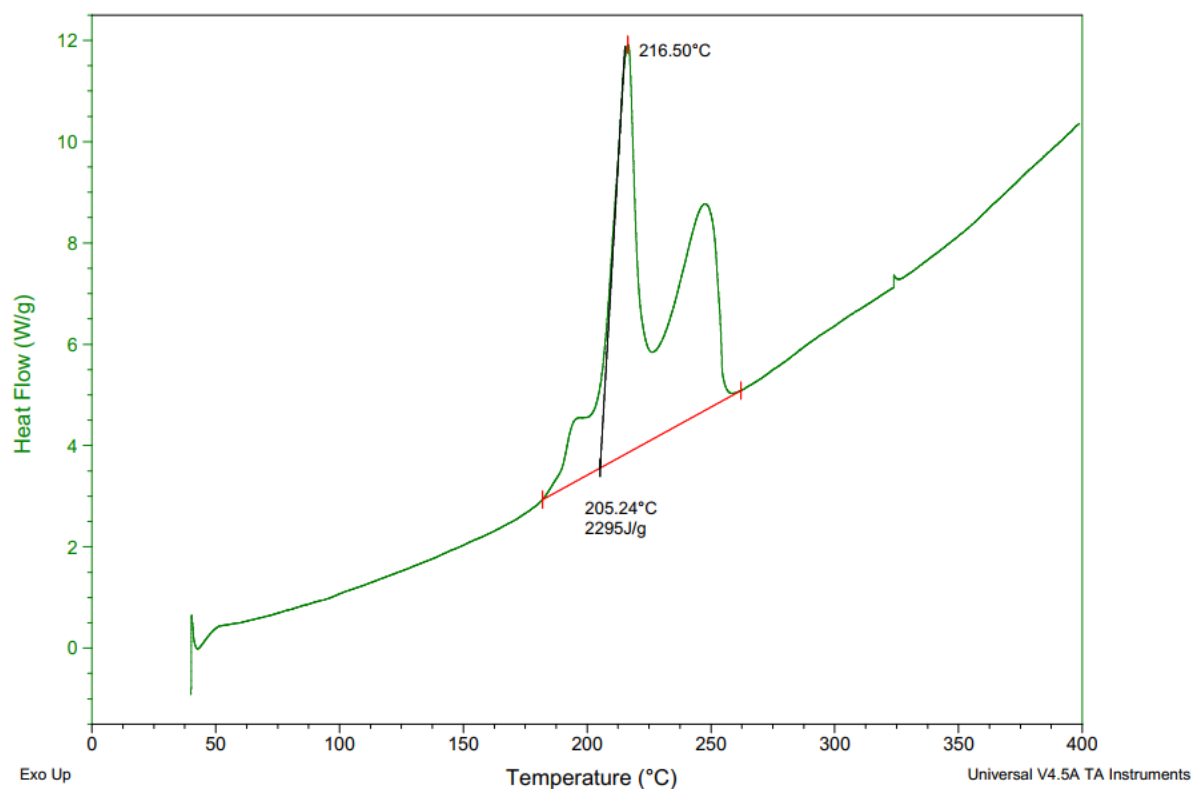


Figure S25. DSC Plot of compound 7 at heating rate 5 °C min⁻¹.

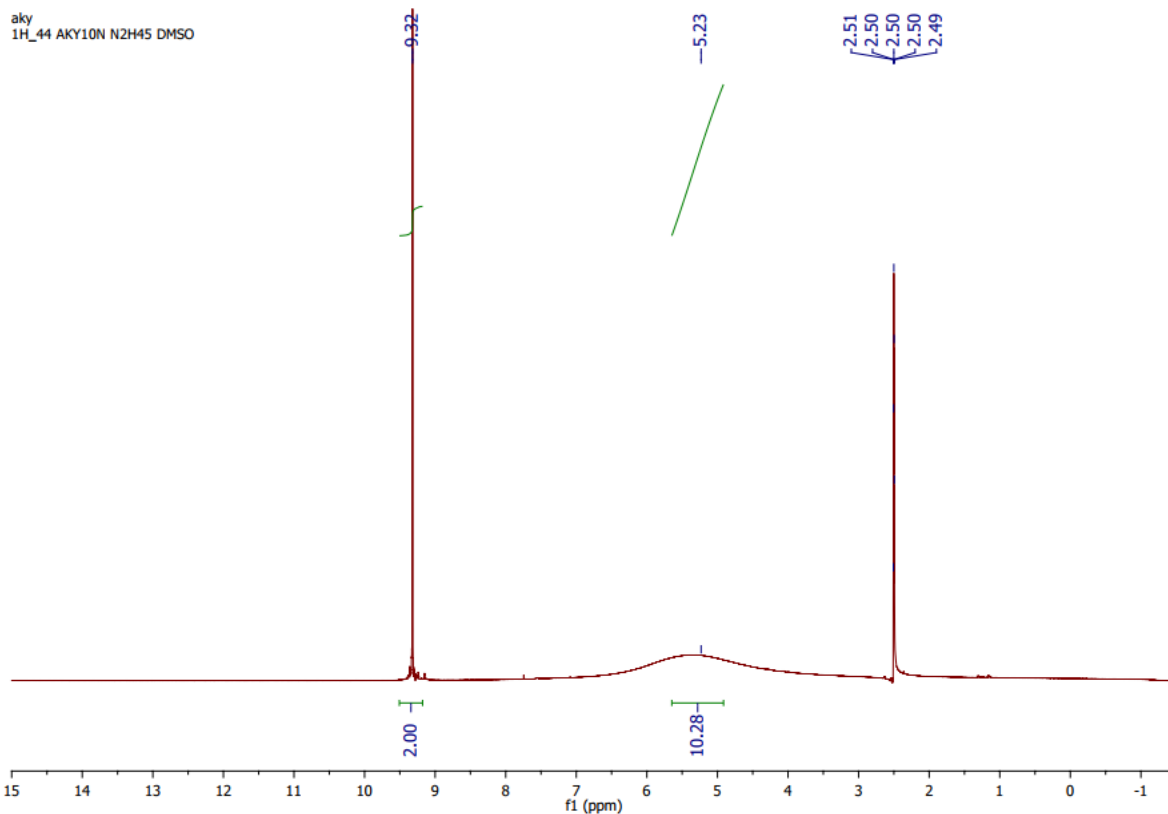


Figure S26: ^1H NMR Spectrum of compound 8 (recorded in DMSO- d_6 ; 500 MHz).

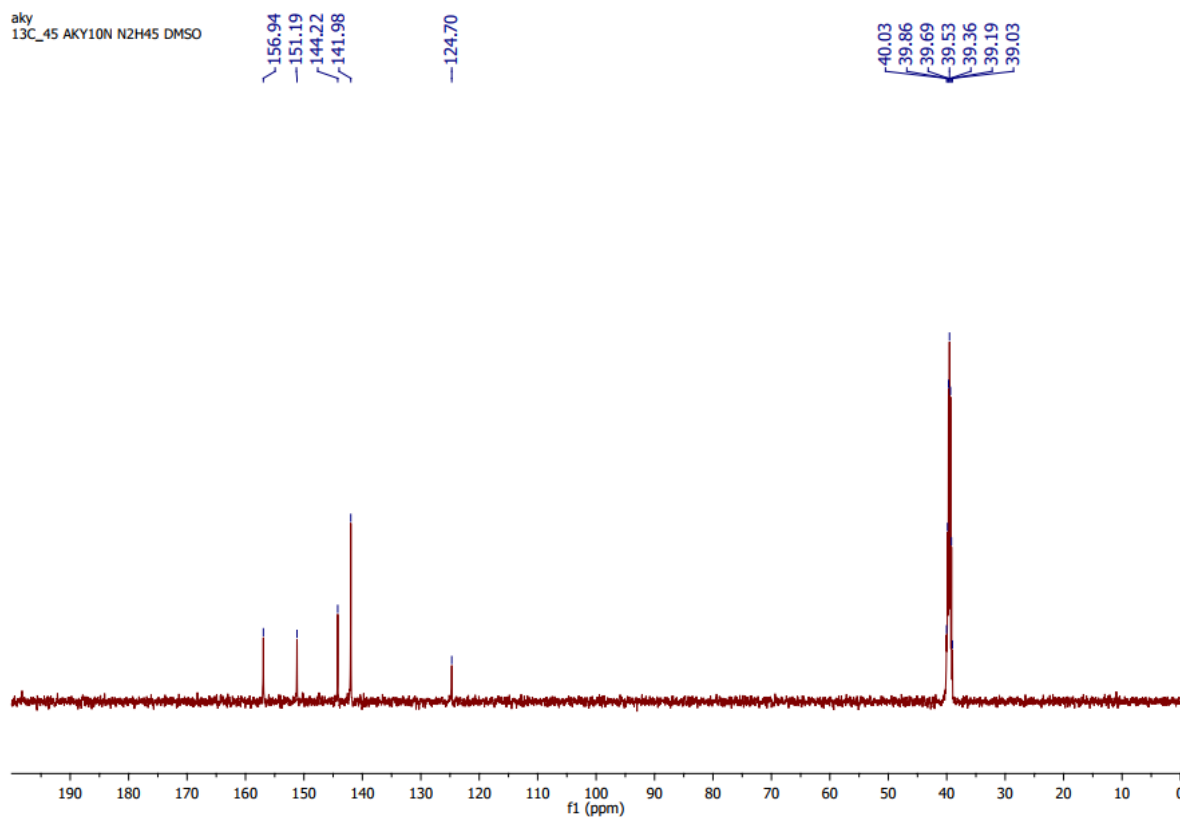


Figure S27: $^{13}\text{C}\{^1\text{H}\}$ NMR Spectrum of compound 8 (recorded in DMSO- d_6 ; 126 MHz).

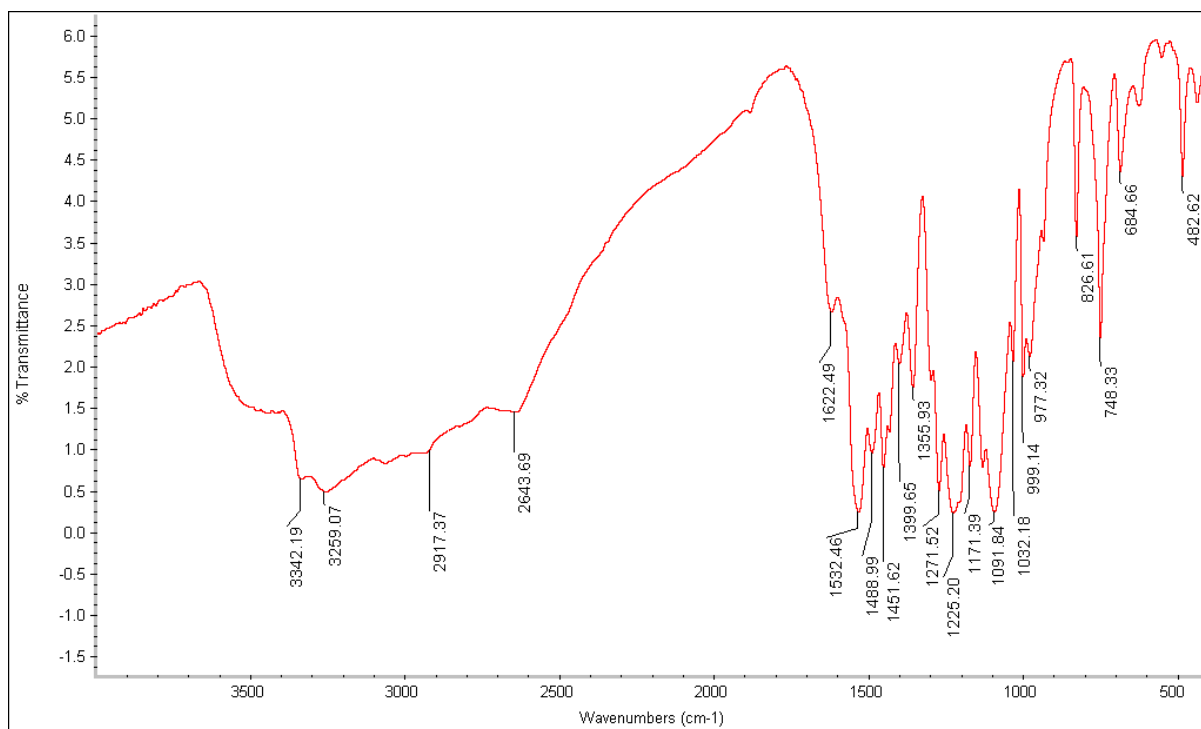


Figure S28: IR Spectrum of compound 8.

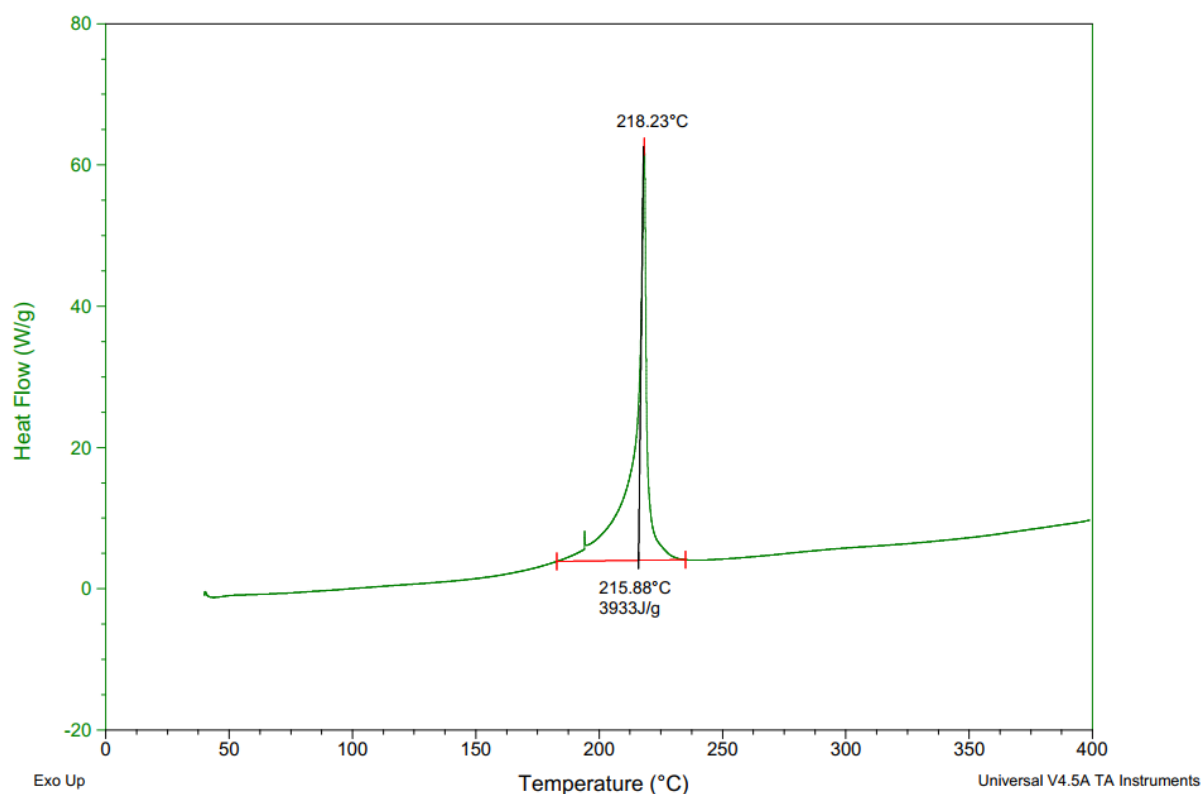


Figure S29. DSC Plot of compound 8 at heating rate 5 °C min⁻¹.

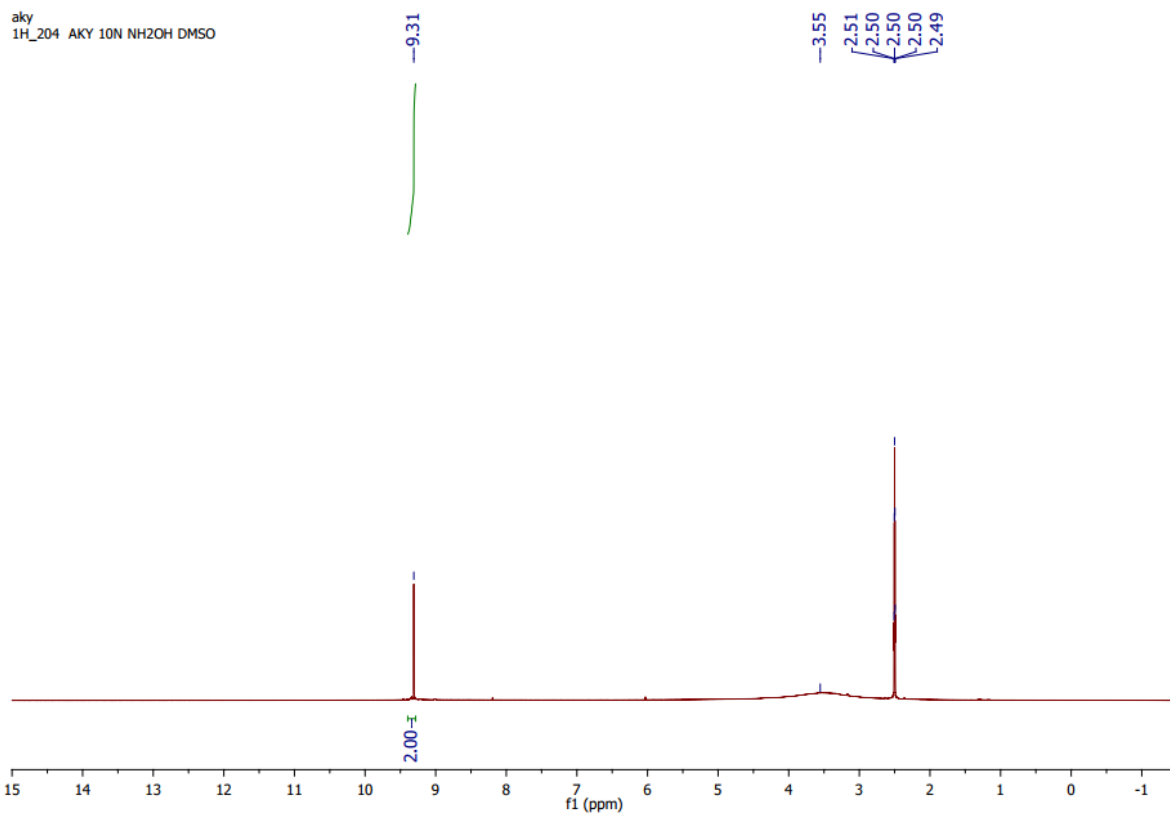


Figure S30: ^1H NMR Spectrum of compound 9 (recorded in DMSO- d_6 ; 500 MHz).

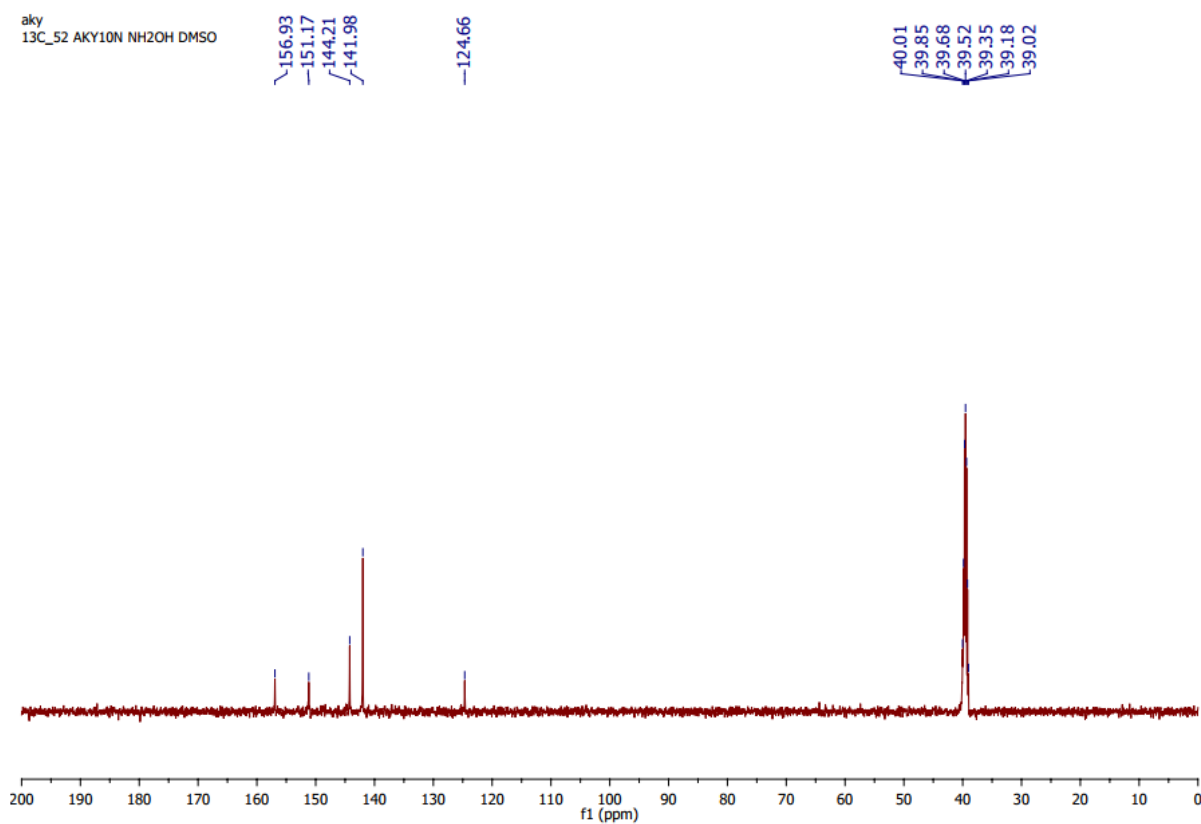


Figure S31: $^{13}\text{C}\{^1\text{H}\}$ NMR Spectrum of compound 9 (recorded in DMSO- d_6 ; 126 MHz).

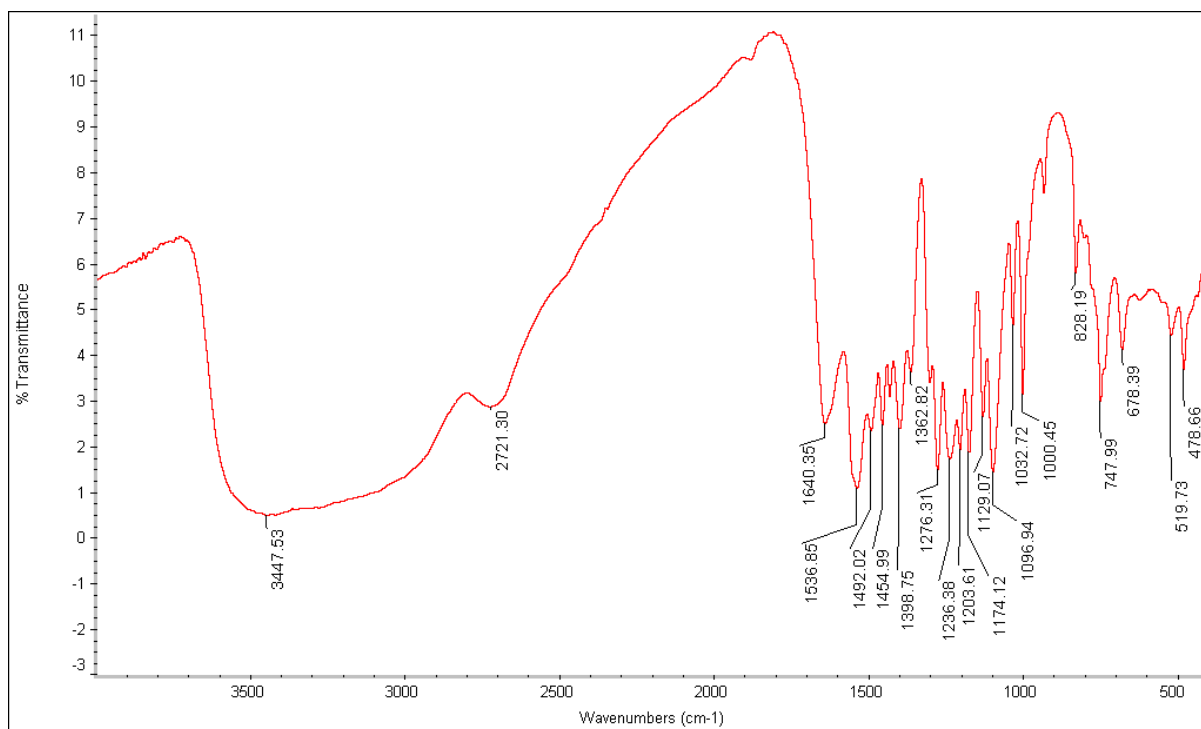


Figure S32: IR Spectrum of compound 9.

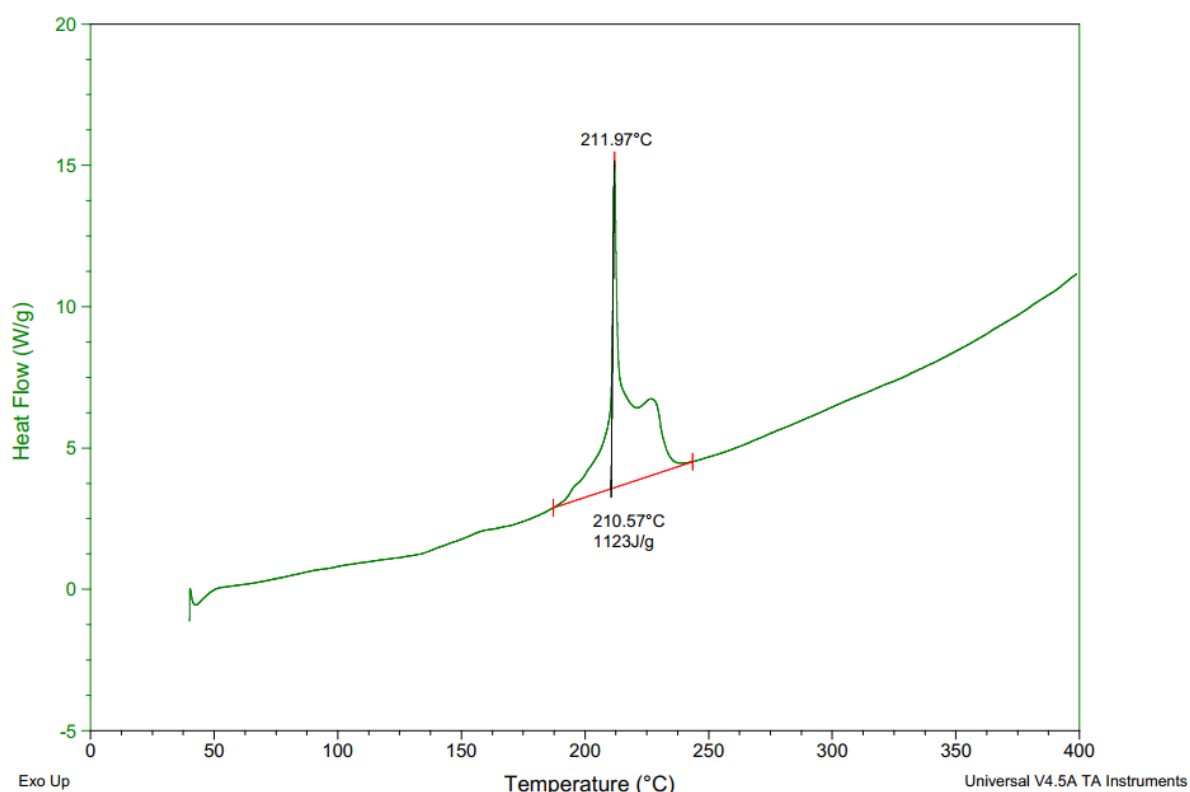


Figure S33. DSC Plot of compound 9 at heating rate 5 °C min⁻¹.

Computational details

Calculations of the heats of formation were carried out using Gaussian 09 suite of programs.⁴ Compound 5, and the anion of 5 were determined using isodesmic reactions (Scheme S1). The

geometric optimization and frequency analyses of the structures were calculated using B3LYP/6-31+G** level and single energy points were calculated at the MP2/6-311++G** level.⁵ The gas phase enthalpies of formation were computed using isodesmic reactions and the enthalpies of reaction were obtained by combining the MP2/6-311++G** energy difference for the reactions, the scaled zero-point energies (ZPE), values of thermal correction (HT), and other thermal factors (**Table S2**). The atomization energies for cations were calculated by using the *G²ab initio* method.⁶ The solid-state heat of formation for neutral compound (**5**) was calculated by subtracting the corresponding enthalpy of sublimation (ΔH_{sub}) from the gas phase enthalpy as shown in equation 1. The heat of sublimation was obtained using Trouton's rule⁷ as shown in equation 2, where T represents either the melting point or the decomposition temperature when melting does not occur prior to decomposition.

$$\text{HOF}_{\text{solid}} = \text{HOF}_{\text{gas}} - \text{HOF}_{\text{sub}} \quad (1)$$

$$\Delta H_{\text{sub}} = 188/\text{Jmol}^{-1}\text{K}^{-1} \times T \quad (2)$$

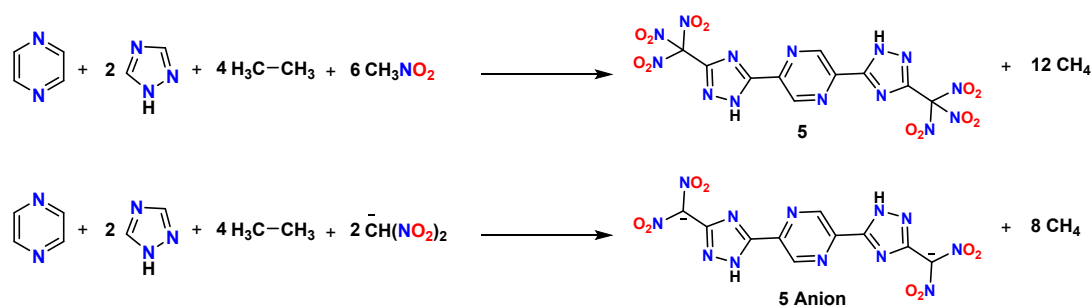
The HOFs of energetic salts were predicted using the Born–Haber cycle (**Figure S34**) and can be simplified by the equation (3),

$$\text{HOF}(\text{salt}, 298 \text{ K}) = \text{HOF}(\text{cation}, 298 \text{ K}) + \text{HOF}(\text{anion}, 298 \text{ K}) - H_{\text{L}} \quad (3)$$

In the above equation, H_{L} is the lattice energy of the salts (see **Table S3**), which can be predicted by using the formula proposed by Jenkins et al.⁸

$$H_{\text{L}} = U_{\text{POT}} + [p(\frac{n_{\text{M}}}{2} - 2) + q(\frac{n_{\text{X}}}{2} - 2)]RT \quad (4)$$

The nature of the cation M_{p}^{+} and anion X_{q}^{-} decide n_{M} and n_{X} values, respectively and are equal to three for monoatomic ions, five for linear polyatomic ions, and six for nonlinear polyatomic ions. U_{POT} is the lattice potential energy, calculated using the density (ρ in g/cm^3) and the chemical formula mass (M in g/mol) of the ionic salt.



Scheme S1. Designed isodesmic reactions for the prediction of HOF_{gas} of compound **5** and its anion.

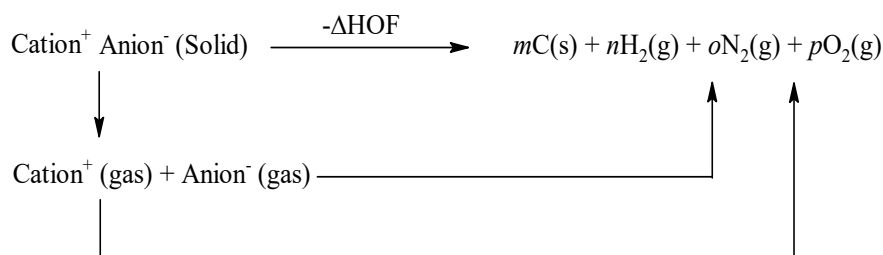


Figure S34. Born-Haber cycle for the formation of energetic salts.

Table S2. Calculated zero-point energies (ZPE), and thermal corrections (H_T) and HOF_{gas} of reference and target compounds at the B3LYP/6-31+G** level and single energy points were calculated at the MP2/6-311++G** level.

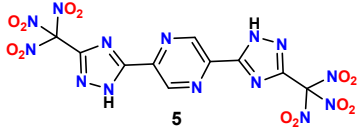
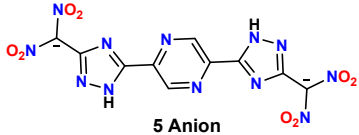
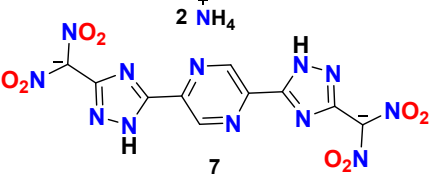
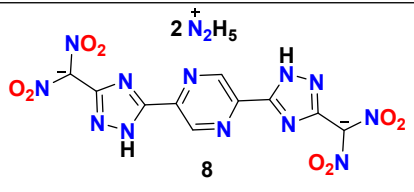
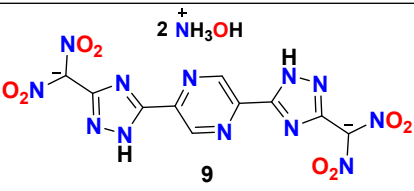
Compd.	ZPE (au)	H_T (au)	Mp-6-311++g**	HOF_{gas} (kJ/mol)
 5	0.223907	0.031295	-2047.587917	575.4421746
 5 Anion	0.196313	0.025186	-1638.329828	196.12325

Table S3. Energy content of energetic salt **7-9**.

Salt	HOF_c^a	HOF_a^b	H_L^c	$\text{HOF}_{\text{salt}}^d$
 7	626.4	196.1	1168.976	279.94

 <p style="text-align: center;">8</p>	770	196.1	1145.461	590.63
 <p style="text-align: center;">9</p>	669.5	196.1	1139.032	396.06

^aHeat of formation of cation (kJ mol⁻¹). ^bHeat of formation of anion (kJ mol⁻¹). ^cLattice energy (kJ mol⁻¹). ^dHeat of formation of salt (kJ mol⁻¹).

References:

1. G. M. Sheldrick, *Acta Cryst.* 2008, **A64**, 339-341.
2. G. M. Sheldrick, *Acta Crystallogr. Sect. A Found. Adv.* 2015, **71**, 3-8.
3. O. V. Dolomanov, L. J. Bourhis, R. J. Gildea, J. A. K. Howard and H. Puschmann, *J. Appl. Crystallogr.* 2009, **42**, 339-341.
4. Gaussian 09, Revision E.01, M. J. Frisch, G. W. Trucks, H. B. Schlegel, G. E. Scuseria, M. A. Robb, J. R. Cheeseman, G. Scalmani, V. Barone, B. Mennucci, G. A. Petersson, H. Nakatsuji, M. Caricato, X. Li, H. P. Hratchian, A. F. Izmaylov, J. Bloino, G. Zheng, J. L. Sonnenberg, M. Hada, M. Ehara, K. Toyota, R. Fukuda, J. Hasegawa, M. Ishida, T. Nakajima, Y. Honda, O. Kitao, H. Nakai, T. Vreven, Jr. J. A. Montgomery, J. E. Peralta, F. Ogliaro, M. Bearpark, J. J. Heyd, E. Brothers, K. N. Kudin, V. N. Staroverov, R. Kobayashi, J. Normand, K. Raghavachari, A. Rendell, J. C. Burant, S. S. Iyengar, J. Tomasi, M. Cossi, N. Rega, J. M. Millam, M. Klene, J. E. Knox, J. B. Cross, V. Bakken, C. Adamo, J. Jaramillo, R. Gomperts, R. E. Stratmann, O. Yazyev, A. J. Austin, R. Cammi, C. Pomelli, J. W. Ochterski, R. L. Martin, K. Morokuma, V. G. Zakrzewski, G. A. Voth, P. Salvador, J. J. Dannenberg, S. Dapprich, A. D. Daniels, O. Farkas, J. B. Foresman, J. V. Ortiz, J. Cioslowski, D. J. Fox, *Gaussian, Inc.*, Wallingford CT, 2013.
5. R. G. Parr, Y. Weitao, *Density-Functional Theory of Atoms and Molecules*; *Oxford University Press*, 1995.
6. O. Suleimenov, T.-K. Ha, *Chem. Phys. Lett.* 1998, **290**, 451–457.
7. M. S. Westwell, M. S. Searle, D. J. Wales, D. H. Williams, *J. Am. Chem. Soc.* 1995, **117**, 5013–5015.

8. H. D. B. Jenkins, D. Tudela, L. Glasser, *Inorg. Chem.*, 2002, **41**, 2364.